Biophysical Journal Volume 65 December 1993 2622–2643

Inner Clot Diffusion and Permeation during Fibrinolysis

Scott L. Diamond and Sriram Anand
Bioengineering Laboratory, Department of Chemical Engineering, State University of New York at Buffalo, Buffalo, New York 14260 USA

ABSTRACT A model of fibrinolysis was developed using multicomponent convection-diffusion equations with homogeneous reaction and heterogeneous adsorption and reaction. Fibrin is the dissolving stationary phase and plasminogen, tissue plasminogen activator (tPA), urokinase (uPA), and plasmin are the soluble mobile species. The model is based on an accurate molecular description of the fibrin fiber and protofibril structure and contains no adjustable parameters and one phenomenological parameter estimated from experiment. The model can predict lysis fronts moving across fibrin clots (fine or coarse fibers) of various densities under different administration regimes using uPA and tPA. We predict that pressure-driven permeation is the major mode of transport that allows for kinetically significant thrombolysis during clinical situations. Without permeation, clot lysis would be severely diffusion limited and would require hundreds of minutes. Adsorption of tPA to fibrin under conditions of permeation was a nonequilibrium process that tended to front load clots with tPA. Protein engineering efforts to design optimal thrombolytics will likely be affected by the permeation processes that occur during thrombolysis.

INTRODUCTION

The biochemistry of thrombolytic therapy for the treatment of acute myocardial infarction has been the subject of intensive study. Plasminogen activators such as tissue plasminogen activator (tPA), urokinase (uPA), or streptokinase (SK) are all currently used clinically to convert plasminogen to plasmin. Plasmin proteolytically degrades the fibrin of the blood clot leading to thrombolysis. A challenge with this type of therapy is the need for rapid reperfusion balanced against the risk of systemic bleeding. With successful thrombolysis, reperfusion times vary from about 20 to 80 min. Generally, about 80 mg of tPA or 10^6 IU (~90 mg) of uPA is administered IV, or about 20 mg of tPA or 0.5×10^6 IU (~45 mg) of uPA is administered locally via catheter over a 1-h period for acute myocardial infarction (*Physicians' Desk Reference*, 1992).

The structures of real blood clots are extremely complicated and variable. During platelet activation, prothrombin is activated to thrombin which then cleaves the negatively charged fibrinopeptides A and B from the central E domain (NH_2 terminals of α and β chains) of fibrinogen, yielding an active fibrin monomer. This monomer rapidly polymerizes end-to-end to form protofibrils of staggered arrangement (for a review, see Doolittle, 1984; and more recently, Weisel and Nagaswami, 1992; Hunziker et al., 1990). The protofibrils can also aggregate side-to-side to form fibers with diameters of about 100 to 500 nm (Carr et al., 1977; Carr and Hermans, 1978; Blomback and Okada, 1982; Blomback et al., 1989; Weisel and Nagaswami, 1992) under physiological conditions. Entrapped platelets can retract the fibrin to about a tenth of the original volume by squeezing plasma from the clot. Clot retraction occurs if the clot boundary is allowed to move. Otherwise an isometric force is generated on the fixed boundary by the clot (Jen and McIntire, 1986). Retracted clots are particularly resistant to fibrinolytic degradation (Sabovic et al., 1989) possibly due to the reduction of the fluid phase plasminogen in the clot. Arterial thrombi which can be flow-compacted may contain an even more dense network of fibrin. Thrombin-activated Factor XIIIa can crosslink the protofibrils and fibers through transamidase activity which catalyzes the formation of ϵ-(γ-glutamyl)lysine bonds between α chains or γ chains of adjacent fibrin monomers to yield α-polymers and γ-dimers. Under physiological conditions, the γ-γ crosslinks are formed at a faster rate than the α-α crosslinks. During lysis of the fibrin gels many different fibrin degradation products are produced. In noncrosslinked gels, the intermediate X and Y fragments can be degraded further to E and D fragments, while in crosslinked gels, fragments contain significant quantities of D-D dimers.

The physical and biochemical structure of the fibrin clot depends upon the polymerization conditions such as the thrombin concentration, the fibrinogen concentration, the ionic strength of the solution phase, and the hemodynamic environment (Carr et al., 1977; Weisel and Nagaswami, 1992). The gel structure is made of long fibrin fibers with relatively uniform diameters. Branching is often observed (Blomback et al., 1989). Fibrin gels formed under low ionic strength (0.1 mM) display more lateral aggregation of protofibrils compared to those formed under high ionic conditions (0.3 mM) which kinetically favors protofibril extension. The fiber diameter is thick (100–500 nm) in coarse gels formed at low ionic strength, while fine gels formed at high ionic strength have a typical fiber diameter of about 8 to 100 nm. Also, the specific permeability is much higher in coarse gels of clotted plasma ($k \sim 10^{-8}$ cm^2) than in fine gels of clotted plasma ($k \sim 10^{-10}$ cm^2) (Carr et al., 1977; Carr and

Received for publication 17 June 1993 and in final form 2 September 1993.

Address reprint requests to Dr. Scott L. Diamond, Bioengineering Laboratory, Department of Chemical Engineering, School of Engineering and Applied Sciences, Clifford C. Furnas Hall, State University of New York at Buffalo, Buffalo, NY 14260.

Abbreviations used: tPA, tissue plasminogen activator; uPA, urokinase; plg, plasminogen; plm, plasmin; fbn, fibrin; PAI-1, plasminogen activator inhibitor type 1; FDP, fibrin degradation products.

0006-3495/93/12/2622/22 $2.00

Hardin, 1987; Blomback et al., 1989). In flow-compacted coarse fibrin (~220 μM fibrin; porosity ~ 0.75), the specific permeability may be as low as 10^{-11} cm^2 or less. The effective pore diameter is on the order of a few microns (3 to 10 μm) in coarse gels of clotted plasma, while the pore diameter may be as low as 0.1 to 0.5 μm in fine gels. In purified fibrin gels or retracted blood clots, the pore diameters are relatively large and are not expected to hinder the Brownian motion of soluble proteins (Brenner and Gaydos, 1977; Blum et al., 1989; Phillips et al., 1990; Matveyev and Domogatsky, 1992).

The intent of the present work was to study the impact of inner clot transport phenomena on the fibrinolytic system. The diffusion of proteins through polymeric gels such as fibrin is a relatively slow process compared to permeation. In the absence of fluid permeation through the clot, the lysis front moving across a clot cannot proceed faster than diffusion. Hundreds of hours would be required for a protein to diffuse a distance of 1 cm. If the therapeutic dose of 1.0 mg of tPA were instantaneously distributed and bound to a 1-ml clot (formed from 3 mg of fibrinogen) which contained 0.075 μM plasminogen (typical clot-bound concentration) over 99% of the plasminogen would be converted to plasmin within a few seconds. Yet for moderately sized clots, substantial lysis does not occur on a time scale of seconds or a few minutes. It is likely that rate limits involved in plasminogen activation, plasmin degradation of fibrin, and transport of plasminogen activators into a clot can prolong the time needed to reperfuse a vessel during thrombolytic therapy. The present study has sought to develop a realistic model of the fibrinolytic pathways in order to identify rate-limiting steps during thrombolytic therapy. The limits of transport likely play an important role in controlling clot lysis.

MODEL FORMULATION

To model the process of fibrinolysis, we have used a system of multicomponent convection-diffusion transport equations with homogeneous reaction and heterogeneous adsorption and reaction (Bird et al., 1960; Rubin, 1983; Kirkner et al, 1984; Whitaker, 1987). The species considered are: tPA, urokinase, plasminogen (glu- or lys-plasminogen), plasmin, and fibrin. These species can reside in either the fluid phase or the fibrin phase of the clot. During the simulations of fibrinolysis, the structural properties of the fibrin evolve in time as the clot is degraded.

Convective transport properties

Little is known about the diffusive and convective transport of proteins through real blood clots. Permeation (also termed: advection, convection, or perfusion) through fibrin is described accurately by Darcy's Law (Eq. 1) for slow, unidirectional flow where the flow rate Q (cm^3/s) per cross-sectional area A (cm^2) is proportional to the pressure drop $\Delta P/L$ (dyne/cm^2 per cm-clot) across the clot (Carr et al., 1977; Blomback et al., 1989). No specific permeability data is available for actual platelet-contracted, flow-compacted blood clots which contain layers of fibrin, platelets, and red blood cells. Using nominal values for a coronary blood clot ($\Delta P/L \sim 60$ mm Hg/cm-clot or 8×10^4 dyne/cm^2 per cm-clot), the superficial velocity v may be as high as 0.001 cm/s.

$$\text{Darcy's Law} \qquad v = \frac{Q}{A} = -\left(\frac{k}{\mu}\right)\frac{\Delta P}{dL} \tag{1}$$

The specific permeability of a fibrous medium is often correlated with the overall porosity and a length scale of the microstructure such as fiber diameter. We have found that the Davies' equation (Dullien, 1979) (Eq. 2) accurately correlated the data of Blomback (1989) for permeability measurements made on fibrin gels polymerized under various thrombin concentrations and ionic strengths. In their study, the overall fibrin porosity was calculated by Blomback et al. (1989) for hydrated fibrin strands while the fiber diameter was determined by three-dimensional confocal microscopy and permeation experiments.

Davies' Equation

$$k = \frac{D_{\text{fiber}}^2}{70(1-\epsilon)^{3/2}\{1 + 52(1-\epsilon)^{3/2}\}} \tag{2}$$

In uniform fibrin gels, viscous fingering is not expected since the permeating buffer or plasma has nearly the same viscosity as the plasma being displaced from the interstitial regions of the clot. However, the nonisotropic nature of real clots, with layers of platelet-rich and platelet-poor regions generated during the formation of the clot, may lead to preferred channels of perfusion. Retracted platelet-rich regions of the clot which are resistant to flow can direct fluid through more permeable regions of the clot. This spatial variations in clots has been described histologically (lines of Zahn), however this type of clot heterogeneity has not been considered in the present work.

Diffusive/dispersive transport properties

In general, the diffusion of proteins within polymeric gels can be altered by solvent viscosity η and molecular caging by the polymer strands. Since the porosity of pure fibrin is high ($\epsilon > 0.90$), excluded volume effects are expected to be small. Typically, hindered diffusion occurs when the hydrodynamic radius of the protein r_i exceeds about 0.3 of the effective pore radius r_{pore} (Brenner and Gaydos, 1977; Blum et al., 1989; Phillips et al., 1990). The volume-averaged, effective diffusion coefficient of the ith species in fibrin is given as

$$\mathbf{D}_{i,\text{fibrin}}^{\text{eff}} = \text{funct}\left(\frac{r_i}{r_{\text{pore}}}\right) \cdot \left(\frac{\eta_w}{\eta_{\text{plasma}}}\mathscr{D}_i^w\right) \tag{3}$$

where $\text{funct}(r_i/r_{\text{pore}}) = 1$ for $r_i/r_{\text{pore}} < 0.3$ and $\mathscr{D}_i^w$ is the diffusion coefficient of the ith species in water. In coarse gels, the effective pore diameter is about 1 to 5 μm; the correction factor for hindered diffusion is equal to one since

the hydrodynamic radius of most proteins is under 20 nm. In fine gels formed under high ionic strength conditions, the pore radius is as small as 100 nm and a slight hindrance of diffusion of large soluble proteins could occur. In the present work, the correction factor for hindrance is set to unity in agreement with recent studies of protein penetration into retracted clots (Matveyev and Domogatsky, 1992; Park et al.; 1988).

Due to binding interaction with the fibrin network, a protein can display an apparent diffusion much lower than that expected for the protein in a pure plasma phase. Even in the presence of fluid permeation, this binding interaction can severely retard the movement of a protein. Binding interactions of the protein with the fibrin are treated in the overall governing equations of transport (not in Eq. 3) since binding interactions need not be at local equilibrium. This approach allows physical processes (Brownian motion) to be decoupled from biochemical processes such as adsorption and desorption. Strong fibrin binding by a protein will lead to reduced transport as a result of the adsorption terms in the governing equations (Kaufman and Jain, 1990).

With the effective diffusion coefficient containing the appropriate physics, it is possible to define the axial dispersion coefficient which is the sum of molecular diffusion and convection-enhanced mixing across fluid streamlines. Sahimi et al. (1986) describe dispersion as a process occurring in macroscopically homogeneous, microscopically heterogeneous media due to (i) molecular diffusion, (ii) irregular flow paths and mixing through a complex geometry, and (iii) a kinetic mechanism from changing flow speeds in a complex geometry. The tortuosity factor of a fibrous gel of such high porosity as fibrin is estimated to be near unity since fibrin gels have a well-connected pore space. Also, stagnation effects in dead zones are not expected to contribute to the dispersion in uniform fibrin gels because of the well-connected pore space. For this type of dispersion, a common form of the longitudinal dispersion coefficient is $D_L = \alpha_z L_z v^\beta$, where α_z is a geometric parameter typically set to unity, L_z is a characteristic length scale of the microscopic media (such as pore diameter, D_{pore}), and v is the superficial velocity (Sahimi et al., 1986). The exponent β is found experimentally to be between 1 and 2 for most materials, and is set to unity in this work for aperiodic, randomly oriented, fibrous media. Using this formulation, the dispersion coefficient is given in Eq. 4 as a combination of the effective diffusion coefficient and axial dispersion. The contribution of Brownian motion to the dispersion is small when permeation occurs. The Peclet number (Pe) based on the dispersion coefficient is given as $Pe_L = v \cdot L/D_L$ and can range nominally from zero to an order of 10^3 for arterial thrombi. The complex effects of adsorption and reaction on the dispersion coefficient are not considered since dispersive phenomena has a relatively smaller contribution toward overall fibrinolysis for $Pe_L > 1$.

$$\mathbf{D}_L^{i,\text{fibrin}} = \mathbf{D}_{i,\text{fibrin}}^{\text{eff}} + \mathbf{D}_{\text{pore}}\mathbf{v} \tag{4}$$

Protein adsorption

When considering an appropriate description for the adsorption of molecules from the plasma phase of a fibrin gel on to the actual fibers of the fibrin, each species must be considered individually. In general, adsorption can be: (i) at local equilibrium between the fluid and fibrin phase, (ii) kinetically-controlled by the forward and reverse rate of adsorption and desorption, or (iii) controlled by mass transfer limits across stagnant boundary layers (Rubin, 1983).

In situations of significant permeation, the strong connectivity of fibrin structures (especially in purified fibrin gels) would produce liquid convection through much of the pore space with little space remaining unperfused. Very near fiber strands, domains may exist which are poorly mixed. Although the pore size in clots and gels is relatively large (on the order of a micron) and does not significantly hinder diffusion (Matveyev and Domogatsky, 1992), the time necessary for a protein to diffuse across a pore is relatively small. For a typical protein with a diffusion coefficient of 5×10^{-7} cm^2/s in the water phase of the gel, it would require a characteristic time well under a second to move across the pore. A stagnant film at the fiber surface is unlikely to pose much of a limit on transport since diffusion can achieve mixing on lengths of a micron and times of a second. More formally, in the worst case scenario in a gel pore with maximum forward rate adsorption to fully available sites {max. forward rate $= (k_f\ \theta_i) \cdot C_{bulk}$} with transport only by Brownian motion, the Damkohler number ($N_{Da} = [(k_f\ \theta_i)\ D_{pore}{}^2/D_i^{eff}]^{1/2}$) is less than 0.01 for plasminogen, plasmin, and tPA adsorption to fibrin. For $N_{Da} < 0.1$, adsorption phenomena is kinetically controlled and is not diffusionally controlled (Bischoff, 1965). Thus, when applying continuum models to understand adsorption during fibrinolysis, it is an accurate approach to assume kinetically-controlled adsorption. If the forward and reverse rates of adsorption are high and of similar magnitude, then the kinetically-controlled adsorption formulation would result in local equilibrium.

We model the kinetically controlled adsorption of a soluble species to fibrin by a second order forward rate constant (k_f, $\mu M^{-1}\ s^{-1}$) describing the association between free solute and available binding sites. Available binding sites are defined as the total concentration of the ith site θ_i minus the concentration of these site which are filled. A first order reverse rate constant (k_r, s^{-1}) describes the dissociation of bound species. The net rate of change of bound concentration of the ith species is

$$\frac{\partial c_i^b}{\partial t} = k_f c_i^f(\theta_i - c_i^b) - k_r c_i^b \tag{5}$$

The parameters for the adsorption of tPA, plasminogen and plasmin are given in Table 1. At a given position in the clot, the bound concentration c_i^b is defined as the moles of the ith species contained within the local fibrin solid phase volume. For equilibration with fibrin of the ith species at $c_i(o)$ initially in the fluid phase, conservation of mass requires that $c_i^f +$

TABLE 1 Summary of kinetic parameters for the reversible adsorption and desorption of plasminogen (plg) and tissue plasminogen activator (tPA) to fibrin

Reversible adsorption	Kinetic constants	Reference
fbn + $plg^f \rightleftharpoons plg^b$	glu-plasminogen $K_d = 38\ \mu M$ $k_f = 1.087 \times 10^{-4}\ \mu M^{-1}s^{-1}$ * $k_r = 4.131 \times 10^{-3}\ s^{-1}$	Lucas, et a. (1983) ($q_{glu\text{-}plg} = 2.0$ sites/monomer)
	lys-plasminogen $K_d = 0.5\ \mu M$ $k_f = 1.087 \times 10^{-4}\ \mu M^{-1}s^{-1}$* $k_r = 5.435 \times 10^{-5}\ s^{-1}$	Lucas, et al. (1983) ($q_{lys\text{-}plg} = 2.4$ sites/monomer)
fbn + $plm^f \rightleftharpoons plm^b$	glu-plm or lys-plasmin $K_d = 0.5\ \mu M$ $k_f = 1.087 \times 10^{-4}\ \mu M^{-1}s^{-1}$‡ $k_r = 5.435 \times 10^{-5}\ s^{-1}$	Suenson & Thorsen (1981) ($q_{plm} = 2.0$ sites/monomer)
fbn + $tpa^f \rightleftharpoons tpa^b$	$k_d = 0.58\ \mu M$ $k_f = 1.148 \times 10^{-4}\ \mu M_{-1}s^{-1}$§ $k_r = 6.658 \times 10^{-5}\ s^{-1}$	Husain, et al. (1989) ($q_{tpa} = 1.5$ sites/monomer)

Urokinase was assumed to have no binding interaction with fibrin (f = free, b = fibrin bound).

* Calculated for 1.65 μM of free lys-plasminogen binding to dispersed (sonicated) fibrin which required a time of 10 minutes to reach equilibrium (Lucas, et al., 1983). It was assumed that glu-plasminogen binds fibrin at the same forward rate as lys-plasminogen. Other reports of plasminogen binding to undispersed fibrin (Bok and Mangel, 1985; Sobovic, et al., 1990) that estimated the time to reach equilibrium to be between 4 to 16 h may contain significant diffusion limited phenomena due to the dense structures and long diffusion lengths. We have assumed that all plasminogen binding sites are available in dispersed fibrin.

‡ Plasmin (either glu-plm or lys-plm) was assumed to complex with fibrin at a forward rate similar to lys-plasminogen binding. This is in part justified by the similar K_d found experimentally for active site-inhibited glu-plasmin and lys-plasmin binding to fibrin (Suenson and Thorsen, 1981).

§ Estimated for 0.005 to 0.75 μM of free single chain tPA binding to 0.135 μM of dispersed (sonicated) crosslinked fibrin which required a time of 15 min to reach equilibrium. We have assumed that all tPA binding sites are available in the dispersed fibrin.

$[(1 - \epsilon)/\epsilon]c_i^b = c_i(o)$. Note, however, that $c_i^f + c_i^b \neq c_i(o)$ in this formulation due to the definition of c_i^b.

Fibrin structure during lysis

Some idealization of the fibrin structure, either in real clots or purified fibrin gels, is needed in order to relate local, instantaneous reaction rates to the evolution of the fibrin structure during lysis. As the fibrin structure undergoes lysis, the void volume (plasma phase) increases. By modeling the evolution of the average local fiber diameter as a function of the local lysis history, it is possible to relate the transport phenomena with the time and space dependent reactions. We model the lysis of the fibrin fiber as a process where plasmin-mediated lysis moves from the outside of the fiber inward, reducing the fiber diameter as lysis proceeds (Fig. 1 *A*). As the clot is lysed, the fiber diameter decreases, while the porosity and subsequently the specific permeability (see Eq. 2) increase. This assumption is justified by the work of Gabriel (1992) which showed the mass-to-length ratio to decrease with time of lysis. However, coarse fibers are known to undergo substantial inner fiber lysis before breakup (Carr et al., 1992). To adequately model both surface and inner fiber lysis would be very difficult and would require: (i) the definition of an inner fiber free and inner fiber bound concentrations as a function of fiber radial position, axial clot distance, and time; (ii) prediction of inner fiber diffusion coefficients; and (iii) simultaneous solution of the radial diffusion/adsorption/reaction equations (in cylindrical coordinates for the fiber) coupled with global transport equations. Our approach takes no account of the branching and crosslinked nature of fibrin, thus rheological information about the elasticity of the gel during lysis is not recovered.

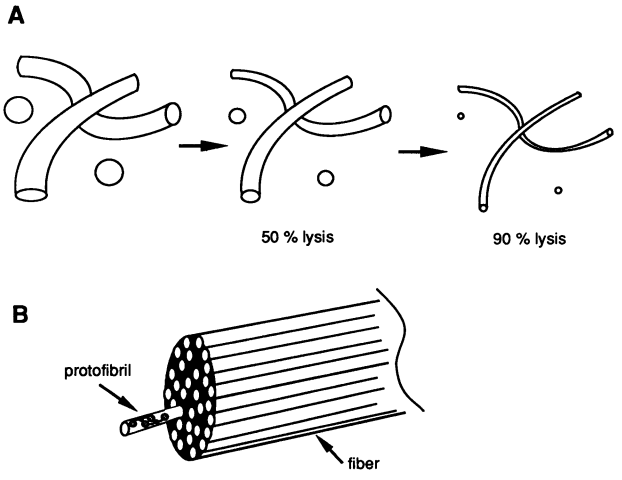

FIGURE 1 (*A*) Schematic model depicting the dissolving of fibrin fibers by plasmin degradation. As the fibers are lyzed, the diameter of the fiber decreases while the length of the fiber remains constant, i.e. lysis of the fiber proceeds radially inward. (*B*) Each fiber is a bundle of many protofibrils. The protofibril is a staggered arrangement of fibrin monomers. Protofibrils on the outer surface of the fiber specifically bind soluble species such as tPA, plasminogen, and plasmin. In the present work, the surface concentration of binding sites and cleavable fibrin sites is calculated from the number of protofibrils on the outer surface of the fiber.

In order to characterize the available binding sites for tPA, plasminogen and plasmin, only protofibrils on the outside of

the fiber were considered sterically accessible for binding of soluble proteins (Fig. 1 *B*). To describe plasminogen activation and plasmin degradation events localized at the surface of the fibrin fibers, it was necessary to evaluate the number of protofibrils exposed on the outside of each fiber. The concentration (θ_i, μM) of binding sites and lytic sites was then related to the number of protofibrils sterically accessible, the number of fibrin monomers per unit length of fibril (about 2 monomers/45 nm or 1.5×10^{11} Da/cm) (Carr et al., 1977; Hunziker et al., 1990), and number of individual sites per monomer (q_i). In this approach of steric accessibility, the tPA and plasminogen adsorption rates are dependent on the available binding sites on the outside of each fiber. Also, the kinetic description of plasmin degradation is dependent on the number of available degradation sites on the outside of each fiber undergoing lysis. As the clot degrades the number of available sites per unit volume decreases.

To calculate the number of protofibrils on the outside of a given fiber of radius, R_f, we assumed that the protofibrils randomly pack with no overlap to yield a final fiber porosity of $\epsilon_{fiber} = 0.80$ and a final fiber density of 0.28 gr-fibrin/ml-fiber (Carr and Hermans, 1978). Using this experimentally determined fiber density, the protofibril probability density, p_o = number of fibrils per cross-sectional area of fiber $= N_o/(\pi R_f^2)$ is given as: $p_o = 0.01116$ fibrils per nm^2 of fiber cross-section (see Appendix). This corresponds to 197 protofibrils in a 150 nm diameter fiber which is consistent with Weisel and Nagaswami (1992). This approach segregates the water in the molecular interstitial regions of the protofibril as part of the void volume of the fiber and not part of the protofibril volume. We evaluated the average number of outer fibrils, m(r), lying at or on the outer radius R_f (Eq. 6). A value of $r_o = 2.39$ nm was used as the average radius of the protofibril which yields a fiber porosity of 0.8 and fiber density of 0.28 gr-fibrin/ml-fiber.The radius of a hydrated protofibril which includes bound water is about 3 to 5 nm. Also, we calculated the number of fibrils, N enclosed within a given fiber radius (Eq. 7) or, inversely, the fiber radius R_f of a bundle of N protofibrils (Eq. 8). See Appendix for details.

$$m(R_f), \quad \text{no. of outer protofibrils on } R_f = [4\pi p_o r_o] \cdot R_f \quad (6)$$

$$N(R_f), \quad \text{no. of protofibrils within } R_f = [\pi p_o] \cdot (R_f)^2 \quad (7)$$

$$R_f, \quad \text{radius of fiber} = [\pi p_o]^{-1/2} \cdot (N)^{1/2} \quad (8)$$

This approach allows the formulation of intrinsic kinetics and adsorption phenomena on an available site basis, instead of macroscopic volume-averaged site concentrations which may not be valid for fibrin of various structures, but same overall concentration. Thus, for a small volume of clot ΔV with length $L_{\Delta V}$ of fibers (see Appendix) of average radius R_f, the fiber surface concentration of a particular site available for reaction or adsorption is defined in Eq. 9 where q_i is the number of the ith site on each fibrin monomer and N_{av} is the Avogadro constant. In general, q_i can be a function of the extent of local lysis if binding sites are revealed in nicked fibrin. The sites may be filled, however, and are then unavailable for adsorption.

$$\theta_i, \mu\text{M } i\text{th site} = q_i \cdot \{m(R_f)\} \cdot \frac{L_{\Delta V}}{\Delta V} \cdot \frac{2 \text{ fibrin monomers}}{45 \text{ nm}} \cdot \frac{1}{N_{av}} \cdot \frac{(10^6 \ \mu\text{mol/mol})}{(10^{-3} \text{ L/cm}^3)} \quad (9)$$

In this approach, q_i is 2.0 binding sites per monomer for glu-plasminogen and plasmin binding (Suenson and Thorsen, 1981; Bok and Mangel, 1985; Fears, 1989); 1.5 binding sites per monomer for tPA binding (Husain et al., 1989; Higgins and Vehar, 1987), and 10 kinetically favored cleavage sites per monomer for plasmin degradation of fibrin (Pizzo et al., 1973; Ranby and Brandstrom, 1988). See Table 2.

Lysis of fibrin by plasmin

Very little intrinsic kinetic data are available for the molecular level action of plasmin on three dimensional networks of fibrin. Most experiments using ^{125}I-fibrin release yield overall solubilization rates without recovery of fundamental rate constants due to the large distribution of cleavage sites and degradation products generated during lysis (Pizzo et al. 1973; Ranby and Brandstrom, 1988). Ample data exists for the cleavage of small soluble substrates such as H-D-val-leu-lys-*p*-nitroanilide (S-2251) (Robbins et al., 1981), H-D-pro-phe-arg-pNA (S-2302), H-D-val-leu-arg-pNA (S-2266), tosyl-gly-pro-lys-pNA (chromozym-PL), (Lottenberg et al., 1981), and tosyl-arg-methyl ester (TAME) (Robbins et al., 1965). During fibrinolysis, however, very complex kinetic phenomena arise when the insoluble fibrin network is degraded by plasmin. Lysine binding sites for plasmin, plas-

TABLE 2 Summary of kinetic parameters for the activation of plasminogen and the degradation of fibrin (b = bound, f = free)

Irreversible reaction	Kinetic constants*	Reference
$plg^b + tPA^b \rightarrow plm^b$	glu-plasminogen $k_2 = 0.10$ s^{-1} $K_m = 0.16$ μM lys-plasminogen $k_2 = 0.2$ s^{-1} $K_m = 0.02$ μM	Hoylaerts et al. (1982)
$plg^f + uPA \rightarrow plm^f$	glu-plasminogen $k_2 = 3.6$ s^{-1} $K_m = 78$ μM lys-plasminogen $k_2 = 4.6$ s^{-1} $K_m = 3.8$ μM	Lijnen et al. (1989)
$fbn + plm^b \rightarrow FDP$	glu or lys-plasmin $k_2 = 25$ s^{-1} $K_m = 250$ μM	Lottenberg et al. (1981)‡

* Values represent nominal activation rates obtained for plasminogen activation by single or two-chain tPA in the presence of unnicked or nicked fibrin. Similarly, nominal rates are given for plasminogen activation by recombinant two-chain urokinase.

‡ The average kinetic parameters for cleavage of fibrin by plasmin are estimated from synthetic substrates. Parameters are for Eq. 12.

minogen, and tPA are revealed on the C-terminal lysine of cleaved chains of the nicked fibrin (Harpel et al., 1985; de Vreis et al., 1989). Plasmin adsorbs reversibly to fibrin with an association with fibrin which is stronger than glu-plasminogen to fibrin and similar or stronger than lys_{77}-plasminogen binding to fibrin which binds with a $K_d = 0.2$ to 10 μM (Suenson and Thorsen, 1981; Bok and Mangel, 1985). The binding of active site-inhibited glu-plasmin to purified fibrin has been evaluated to have a K_d of 0.5 μM (Suenson and Thorsen, 1981). Once bound, plasmin proceeds to engage in its active site the cleavage sites. Additionally, plasmin may immediately form the activated enzyme-substrate complex as plasmin moves from the solution phase onto the fibrin. In this sense, the active site of plasmin may be considered to facilitate plasmin binding to fibrin. Once bound to fibrin, plasmin can desorb but tends to remain localized to the fibrin phase since it is protected from α_2-antiplasmin inhibition.

We have assumed that fibrin bound plasmin reversibly engages its potential cleavage site. Thus, the kinetic description for the rate of fibrin cutting would follow a Michaelis-Menton description. The reaction velocity should go to zero as the fibrin becomes fully degraded (no cleavage sites or bound plasmin available) and reach a maximum rate in the presence of excess fibrin sites. We have assumed that plasmin cleaves all the potential cut sites of the fibrin monomers at an average rate as shown in Eq. 10.

By evaluation of the instantaneous rate of cutting $\{\mathscr{R}(x', t'), \mu M/s\}$ at some location x' at some time t', it is possible to calculate the historic amount of cutting $\{\zeta(x', t'), \mu M$ of cuts made at x' and $t'\}$. By defining a solubilization factor γ, which relates the number of fibrin monomers solubilized to the number of cuts made, the amount of solubilization or lysis $\{L(x', t'), \mu M$ of fibrin lyzed at x' and $t'\}$ can be defined as a function of the historic amount of cuts made by plasmin at position x'. The solubilization factor has been estimated to be a constant with a value of 0.1. This corresponds to the estimate that for every 10 cleavages by plasmin, an equivalent of one subunit of fibrin is solubilized (Ranby and Brandstrom, 1988). This approach does not account for any dependence of plasminogen activating activity or plasmin activity on the actual radius of the fiber which is known to exist with very thin fibrils (Gabriel et al., 1992).

$$\mathscr{R}(x', t') = \frac{k_2 c^b_{plm}(x', t')\, \theta_{plm}(x', t')}{K_m + \theta_{plm}(x', t')} \tag{10}$$

$$\zeta(x', t') = \int_0^{t'} \mathscr{R}(x', t)\, dt \tag{11}$$

$$L(x', t') = \gamma \cdot \zeta(x', t') \tag{12}$$

The % lysis is defined as

$$\%\ \text{lysis} = L(x', t')/(c_{fbn})_o \quad \text{at } x', t' \tag{13}$$

and the time-evolving fiber radius which decreases with lysis is given as

$$R_f(x', t') = \left[R_{f_o}^2 - \left(\frac{1}{\pi p_o}\right) \left\{ \frac{L(x', t')}{\left(\frac{L_T}{Vol_T}\right) \frac{2 \text{ monomers}}{45 \text{ nm}} \frac{1}{N_{av}} \frac{(10^6\ \mu\text{mol/mol})}{(10^{-3}\ \text{l/cm}^3)}} \right\} \right]^{1/2} \tag{14}$$

The advantage of this approach is the relation of kinetic rates and stoichiometry to the time-evolving gel structure at the molecular level. We have used one phenomenological parameter γ to capture the poorly defined process of release of partially degraded fragments. Although the actual fiber is quite porous with a void fraction of 0.8, binding interaction of penetrating proteins with the protofibrils may likely localize these proteins to the outer domains of the fiber. Our approach does not distinguish between species trapped inside fibers during clotting or species bound to the surface of fibers, but does specify that all lysis occurs on the fiber surface (Fig. 1). It is likely that both surface and inner fiber lysis (Carr and Hermans, 1978; Carr et al., 1992) occur in reality but the relative contributions are not known.

The kinetic parameters for plasminogen activation by bound tPA, solution phase activation of plasminogen by urokinase, and plasmin degradation of fibrin by plasmin are given in Table 2. Given the already complex nature of convection and reaction with a multicomponent heterogeneous system, some simplifications were required prior to exploring more complex systems. We have neglected fluid-phase activation of plasminogen by tPA which is kinetically slow. The inhibitory effects of α_2-antiplasmin and PAI-1 either in solution or on fibrin were not considered. We also have not considered the conversion of single-chain tPA to two-chain tPA or the conversion of prourokinase (single chain-uPA) to two-chain-uPA (urokinase). Additionally, we have not considered the conversion of glu-plasminogen to lys_{77}-plasminogen or the generation of glu-plasmin or lys_{77}-plasmin, although the simulation can use parameters for either glu or lys-plasminogen. We have not considered the generation of binding sites in partially degraded fibrin as lysis proceeds or the modulatory action of fibrin degradation products on enzyme activities. We have neglected the biochemical role of various proteins such as albumin, collagen, fibronectin, heparin, and lipoprotein. Finally, these simulations have focused only on the biochemistry of the major proteins of fibrinolysis without consideration of the many cellular contributions of red blood cells, platelets (Miles and Plow, 1985), neutrophils, or the invading fibroblasts of older clots.

A multicomponent convection/dispersion model of fibrinolysis with heterogeneous adsorption and reaction

Fibrinolytic therapy is intrinsically transient. The time-dependent and space-dependent concentration of various

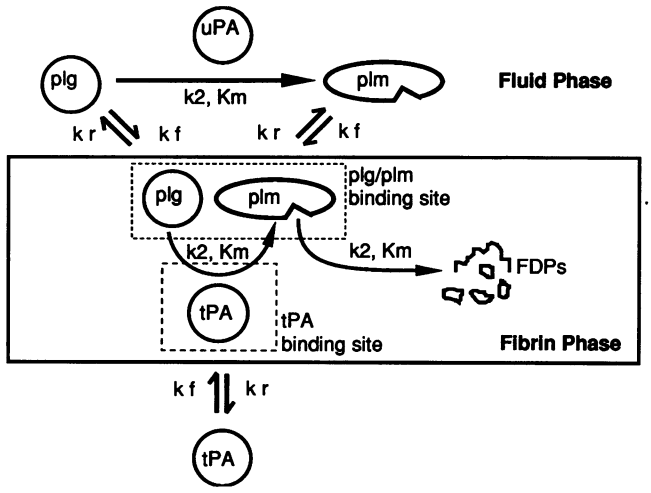

FIGURE 2 Summary of the fibrinolytic reaction pathway and components considered in the model. Plasminogen is activated to plasmin in the solution phase by urokinase while solid phase plasminogen activation requires tPA to be bound to the fibrin. Not included in the present study is the inhibition of soluble plasmin and tPA by α_2-antiplasmin or PAI-1, respectively. Diffusion and convection of soluble species can occur in the fluid phase. Soluble species can reversibly adsorb and desorb to the fibrin phase. Plasminogen and plasmin compete for the same sites on the fibrin monomer. Each site can bind only one molecule at a time. All kinetic constants are given in Table 1 for reversible adsorption and Table 2 for irreversible enzymatic reaction.

species in the fluid and fibrin phase are described by governing Eqs. 15a-d and 16a-d, respectively, and Danckwerts boundary conditions for convection-dominated transport at the clot boundaries (Eq. 17a-b) and initial conditions (Eq. 18) for one-dimensional convective/dispersive transport. The binding of urokinase to fibrin was neglected. The reaction network is summarized in Fig. 2. Plasminogen and plasmin compete for the same site on each fibrin monomer while tPA binds its own unique site (Eq. 16a-b). Plasminogen must be bound to fibrin in order to be activated by bound tPA (Wu et al., 1990). Since all the soluble species have a molecular weight between 50 and 80 kDa, we have used a Brownian diffusion coefficient of 5×10^{-7} cm^2/s for all the soluble species (Tyn and Gusek, 1990; Park et al., 1988). The Brownian contribution in the calculation of the longitudinal dispersion coefficient is quite small for Peclet number much greater than 1. Also, we have neglected in Eq. 15b-c the small amount of urokinase and plasminogen bound temporarily to each other during catalysis.

Numerical solution method

The set of transport equations was solved numerically using a weighted-average finite difference method (Crank-Nicholson method, weight factor = 0.5) with space derivatives averaged over two successive dimensionless time steps of 10^{-6} ($t \cdot L^2/D_L$) (Gupta and Greenkorn, 1973). The spatial domain (1-cm clot length) was discretized with only 11 nodes to provide numerical stability for the multicomponent system. The system was solved on a SUN4 (SUNOS 4.1.2) and required under 5 min of CPU per run. The solution was numerically stable for an initial Peclet number up to about 500. At the start of each run the following parameters were set: initial concentrations, inlet conditions, initial permeation velocity, initial fiber radius. At each time step, the concentration profiles and the local historic amount of lysis $L(x', t')$ were evaluated. Then, the local percentage lysis (Eq. 13), fiber radius (Eq. 14) and porosity were evaluated in order to update the local specific permeability $k(x', t')$ by Eq. 2. The overall permeation velocity at constant pressure drop across the clot was evaluated using the clot-averaged specific permeability. With the updated superficial velocity, new concentrations profiles were evaluated at the next time step. Simulations were stopped as the overall lysis of the clot approached 80% since increasing velocities led to high Pe and associated oscillations in the solution. Adaptive mesh algorithms were not necessary to achieve stable solutions for the Peclet numbers used in the present work. Using refined meshes (25 or 45 nodes) led to longer run times with little gain in numerical stability, but also gave slightly sharper fronts. Thus, with the 11 node mesh, numerical dispersion led to a small over estimation (<15%) of species penetration ahead of the front.

Fluid phase (f = free, b = bound)

$$\text{tPA} \quad \frac{\partial c^{\mathrm{f}}_{\mathrm{tPA}}}{\partial t} = D_L^{\mathrm{tPA}} \frac{\partial^2 c^{\mathrm{f}}_{\mathrm{tPA}}}{\partial x^2} - v \frac{\partial c^{\mathrm{f}}_{\mathrm{tPA}}}{\partial x} - \left(\frac{1-\epsilon}{\epsilon}\right) \frac{\partial c^{\mathrm{b}}_{\mathrm{tPA}}}{\partial t} \tag{15a}$$

$$\text{uPA} \quad \frac{\partial c^{\mathrm{f}}_{\mathrm{uPA}}}{\partial t} = D_L^{\mathrm{uPA}} \frac{\partial^2 c^{\mathrm{f}}_{\mathrm{uPA}}}{\partial x^2} - v \frac{\partial c^{\mathrm{f}}_{\mathrm{uPA}}}{\partial x} \tag{15b}$$

$$\text{plg} \quad \frac{\partial c^{\mathrm{f}}_{\mathrm{plg}}}{\partial t} = D_L^{\mathrm{plg}} \frac{\partial^2 c^{\mathrm{f}}_{\mathrm{plg}}}{\partial x^2} - v \frac{\partial c^{\mathrm{f}}_{\mathrm{plg}}}{\partial x} - \left(\frac{1-\epsilon}{\epsilon}\right) \frac{\partial c^{\mathrm{b}}_{\mathrm{plg}}}{\partial t} - \left(\frac{k_2^{\mathrm{uPA}} c^{\mathrm{f}}_{\mathrm{uPA}} c^{\mathrm{f}}_{\mathrm{plg}}}{K_{\mathrm{m}}^{\mathrm{uPA}} + c^{\mathrm{f}}_{\mathrm{plg}}}\right) \tag{15c}$$

$$\text{plm} \quad \frac{\partial c^{\mathrm{f}}_{\mathrm{plm}}}{\partial t} = D_L^{\mathrm{plm}} \frac{\partial^2 c^{\mathrm{f}}_{\mathrm{plm}}}{\partial x^2} - v \frac{\partial c^{\mathrm{f}}_{\mathrm{plm}}}{\partial x} - \left(\frac{1-\epsilon}{\epsilon}\right) \frac{\partial c^{\mathrm{b}}_{\mathrm{plm}}}{\partial t} + \left(\frac{k_2^{\mathrm{uPA}} c^{\mathrm{f}}_{\mathrm{uPA}} c^{\mathrm{f}}_{\mathrm{plg}}}{K_{\mathrm{m}}^{\mathrm{uPA}} + c^{\mathrm{f}}_{\mathrm{plg}}}\right) \tag{15d}$$

Solid fibrin phase

$$\text{tPA} \quad \frac{\partial c^{\mathrm{b}}_{\mathrm{tPA}}}{\partial t} = k_{\mathrm{f}}^{\mathrm{tPA}} c^{\mathrm{f}}_{\mathrm{tPA}} (\theta_{\mathrm{tPA}} - c^{\mathrm{b}}_{\mathrm{tPA}}) - k_{\mathrm{r}}^{\mathrm{tPA}} c^{\mathrm{b}}_{\mathrm{tPA}} \tag{16a}$$

$$\text{plg} \quad \frac{\partial c^{\mathrm{b}}_{\mathrm{plg}}}{\partial t} = k_{\mathrm{f}}^{\mathrm{plg}} c^{\mathrm{f}}_{\mathrm{plg}} (\theta_{\mathrm{plg/m}} - c^{\mathrm{b}}_{\mathrm{plg}} - c^{\mathrm{b}}_{\mathrm{plm}}) - \mathrm{k}_{\mathrm{r}}^{\mathrm{plg}} c^{\mathrm{b}}_{\mathrm{plg}} - \left(\frac{k_2^{\mathrm{tPA}} c^{\mathrm{b}}_{\mathrm{tPA}} c^{\mathrm{b}}_{\mathrm{plg}}}{K_{\mathrm{m}}^{\mathrm{tPA}} + c^{\mathrm{b}}_{\mathrm{plg}}}\right) \tag{16b}$$

TABLE 3 Physical and biochemical parameters for fibrin clots

Fibrin Structure and Transport Properties	
Fibrin monomer size	45 nm × 6 nm
R_f, radius of fibrin fiber formed at high ionic strength (0.3M)	4 to 50 nm (fine gel)
R_f, Radius of fibrin fiber formed at low ionic strength (0.1M)	200 to 500 nm (coarse gel)
D^{pore}, diameter of pore	0.1 (fine) to 10 μm (coarse)
Overall fibrin porosity, $\epsilon = V_{void}/V_{total}$	>0.99 (plasma gel)
	0.9 - 0.99 (platelet-retracted clots)
	0.75 - 0.9 (flow-compacted fibrin)
Specific permeability	10^{-8} cm^2 (coarse) to 10^{-12} cm^2 (fine)
Peclet number number, Pe = $v \cdot L/D_L$	0 to $\mathcal{O}(10^3)$
$\Delta P/L$	
Arterial	~60 mm-Hg per cm-clot
Venous	0 to 10 mm-Hg per cm-clot

Biochemical constituents	MW (kda)	[conc]plasma	[conc]clot*
tPA	72	0.1 nM	—
uPA	54	0.1 nM	<5%
PAI-1	55	0.2 nM	—
α_2-antiplasmin	67	1.0 μM	~20%
Plasminogen	88 (glu-plg)	2.2 μM	~5–25%
	83 (lys-plg)	—	~50–70%
Plasmin	88 (glu-plm)		
	83 (lys-plm)	$\tau_{1/2}$ ~ 0.1	$\tau_{1/2}$ ~ 10^2 to 10^3
Fibrinogen	340	8.8 μM	—
Fibrin monomer (in clot)		—	8.8 μM (plasma clot)
			88 μM (platelet retracted)
			220 μM (flow-compacted)

* Fibrin bound concentration as percentage of plasma concentration, or half-life ($\tau_{1/2}$) for short-lived species, or μM. During clotting, soluble proteins can also be crosslinked by factor XIIIa such that bound concentrations approach the plasma concentration. These values are consistent with typical values for equilibrium binding to preformed plasma clots or purified fibrin clots.

$$\text{plm} \quad \frac{\partial c^b_{plm}}{\partial t} = k^{plm}_f c^f_{plm}(\theta_{plg/m} - c^b_{plg} - c^b_{plm}) - k^{plm}_r c^b_{plm} + \left(\frac{k^{tPA}_2 c^b_{tPA} c^b_{plg}}{K^{tPA}_m + c^b_{plg}}\right) \quad (16c)$$

Boundary conditions (for free species)

$$\text{Inlet:} \quad vc_{i,inlet} = \left| vc_i - D^i_L \frac{\partial c_i}{\partial x} \right|_{x=0} \quad (17a)$$

for i = tPA, uPA, plg, plm, where

$$c_{i,inlet}(t) = \left\{ \begin{array}{lll} c_i = 0 & \text{for} & t < 0 \quad \text{and} \quad t > t^* \\ c_i = c_{i,bolus} & \text{for} & 0 < t < t^* \end{array} \right\}$$

$$\text{Outlet:} \quad \frac{\partial c_i}{\partial x} = 0 \quad \text{at} \quad x = L_{clot} \; (t > 0) \quad (17b)$$

for i = tPA, uPA, plg, plm

Initial conditions (for bound and free species)

$$c_i(x, t = 0) = c_{i,o} \text{ for } 0 < x < L_{clot} \quad (18)$$

for i = tPA, uPA, plg, plm

RESULTS

For each simulation, the following initial conditions were specified (see Table 3): bulk fibrin concentration, initial fiber radius, initial free and bound plasminogen concentration (in equilibrium with fibrin), and plasminogen subtype used (glu or lys). By setting the pressure drop constant and the concentrations and duration of the bolus perfusion, the problem was specified for each simulation. In certain simulations to illustrate particular phenomena, reaction rates were set to zero or other modifications were made as described.

Penetration and partitioning of proteins in preformed fibrin

To explore the dynamic partitioning of individual species to fibrin under conditions of permeation, the irreversible reactions (Table 2) were all set to zero, corresponding to active-site inhibition. A 0.5-min bolus (finite step input) of 1 μM of tPA, glu-plasminogen, and uPA was administered to a flow-compacted fibrin clot at constant $\Delta P/L$ = 50 mm-Hg/cm (Pe = 421). After 0.5 min, the inlet concentrations were set to zero. Concentration profiles after 30 min of permeation are shown in Fig. 3 for the free and bound concentrations of the penetrating species. Urokinase moved with the permeation front which was located at 0.378 cm after 30 min. The uPA moved ahead of the free tPA and free plasminogen since it had no binding interaction with the fibrin. The mobility of tPA and plasminogen was reduced because of fibrin adsorption. Each component became highly dispersed under these permeation conditions with a small amount of each species moving ahead of the permeation front. The tPA rapidly bound the fibrin of the clot (Fig. 3 *B*), and after 30 min a majority of the tPA was bound to fibrin. For tPA partitioning, a non local equilibrium state occurred-a significant

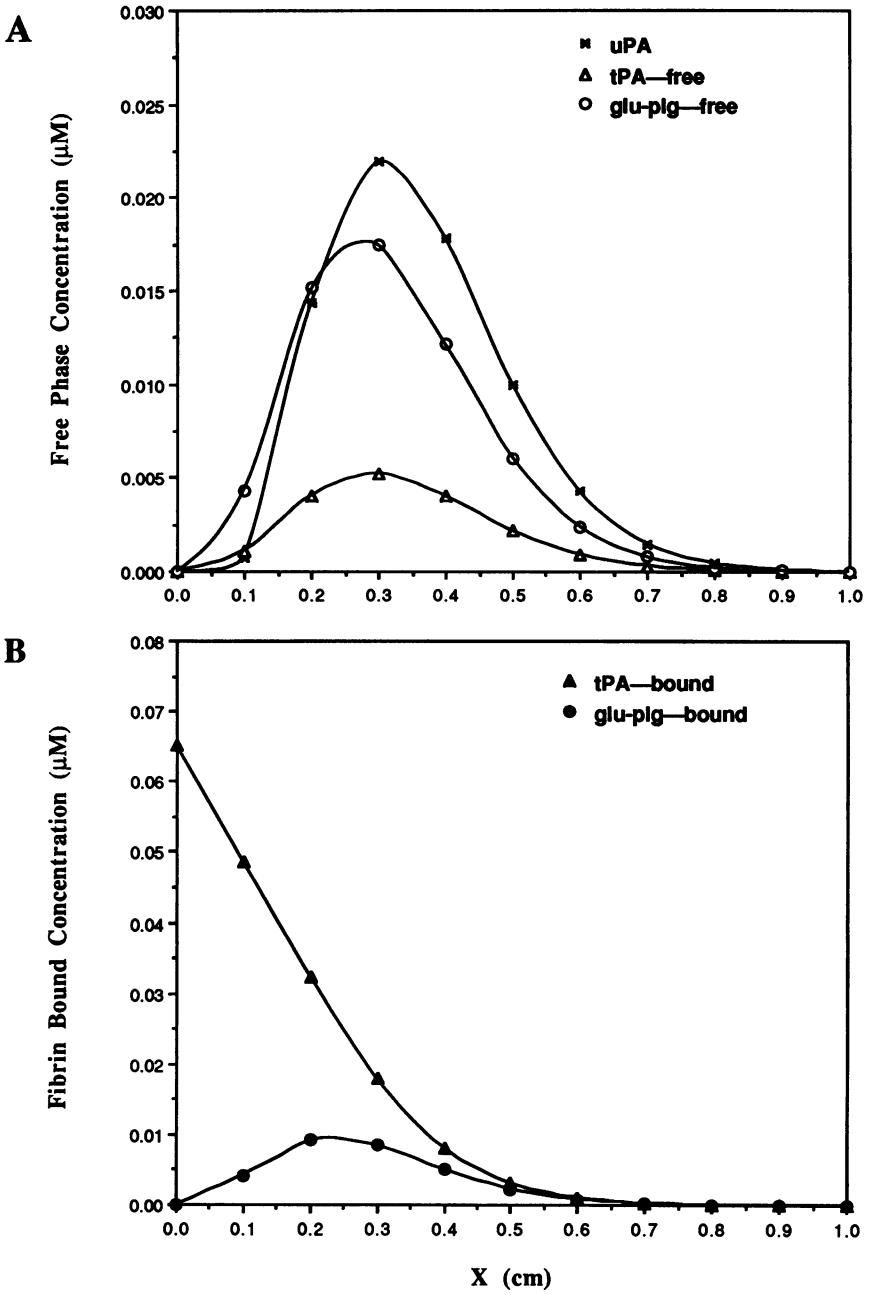

FIGURE 3 The penetration and partitioning of tPA, uPA, and glu-plasminogen (glu-plg) into a coarse (R_{fo} = 250 nm), compacted (220 μM fibrin) clot after 30 min with fluid permeation driven by a constant pressure drop of 50 mm-Hg/cm (Pe = 421). All plasminogen activation and fibrin degradation reaction rates were set to zero, thus no plasmin was generated and the fibrin properties remained constant during the simulation. Inlet concentrations for the 0.5 min bolus were set to 1 μM for each species. (*A*) Free phase concentrations. (*B*) Bound concentrations.

amount of bound tPA at the inlet (x = 0) coexisted with a zero free phase tPA concentration. Local equilibrium would dictate that the concentration of tPA on the fibrin be zero if the solution phase concentration of tPA were zero. Bound glu-plasminogen desorbed from fibrin more rapidly than tPA, and conditions of local equilibrium were more closely approached for the partitioning of glu-plasminogen to fibrin under permeation conditions. In other simulations, the transport of lys-plasminogen and active-site inhibited plasmin occurred under non local equilibrium conditions due to strong fibrin binding.

Plasminogen activation by tPA and lysis under conditions of permeation

When using tPA as a lytic agent, many factors ultimately control fibrin lysis. A typical arterial thrombi would experience a pressure drop across the clot of about 50 mm-Hg/cm-clot. Under this flow condition, a 5-min bolus of 1 μM tPA caused a sharp lysis front to move across a coarse, compacted clot which had been preequilibrated with glu-plasminogen (Fig. 4). Over 80% of the clot was predicted to be lyzed by 45 min. At constant pressure drop, the permeation velocity and the lysis front velocity increased as the clot was lyzed. This is seen in Fig. 4 by comparing the lysis profile at 15 min with the profile at 30 min. This acceleration was due to the accumulation of plasmin with time and the increase of overall clot permeability with lysis.

To demonstrate the fundamental impact of permeation on overall fibrinolysis, simulations were run at different pressure drops of 1, 10, and 50 mm-Hg/cm-clot (Fig. 5 *A*). For lysis of a clot that contained no plasminogen prior to lytic treatment (Fig. 5 *A–C*), the $\Delta P/L$ had a strong effect on lysis. After 15 min of lysis at $\Delta P/L$ = 1 mm-Hg/cm, only the front

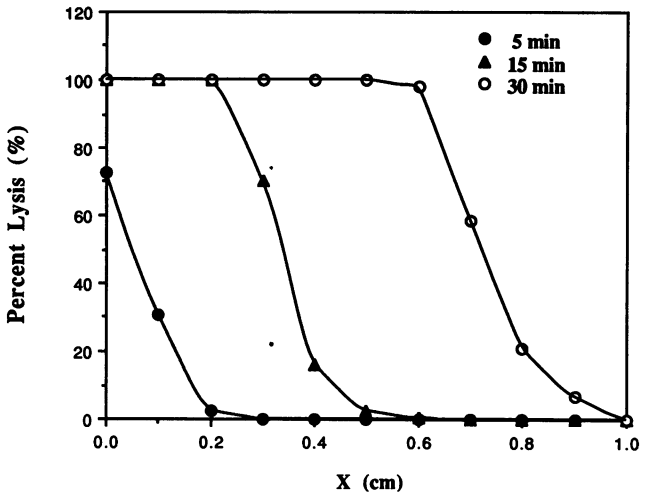

FIGURE 4 Spatial distribution of tPA-mediated fibrinolysis under convective-dispersive transport at various times. Simulations were for lysis of a flow-compacted (220 μM fibrin), coarse (R_{fo} = 250 nm) clot which was pre-equilibrated with 2.2 μM glu-plg (initially, c^b_{plg} = 0.940 μM and c^f_{plg} = 1.856 μM). The permeation was driven by $\Delta P/L$ = 50 mm-Hg/cm (initial Pe = 421 and permeation velocity = 2.10 $\times 10^{-4}$ cm/s). Inlet conditions were: 1.0 μM tPA, 0 μM uPA, 2.2 μM glu-plg, 0 μM plm for a bolus (finite step input) of 5 min, after which all concentrations were set to zero, except for glu-plg, which was maintained at 2.2 μM.

0.1 cm of the clot was slightly lyzed (10%). This was in contrast with nearly 0.2 cm of the clot being highly lyzed at a $\Delta P/L$ of 50 mm-Hg/cm-clot, corresponding to about a 20-fold increase in fibrin solubilization at the higher pressure drop. Although the higher flows led to delivery of more tPA during the 5-minute bolus, similar results were found when a constant mass of tPA was administered at various pressure drops. Thus, the variation in tPA-mediated lysis profiles in Fig. 5 *A* was due to the enhancement of tPA penetration with increasing pressure drop. The bound and free concentrations of each species after 15 min of lysis for constant $\Delta P/L$ = 50 mm-Hg/cm are shown in Fig. 5, *B* and *C*, respectively. Almost all of the plasmin generated on the fibrin by tPA remained bound to the fibrin. Bound concentrations of plasminogen were quite low due to the rapid conversion to plasmin by bound tPA. The bound concentrations of all species at the inlet (x = 0 cm) were zero after 15 min due to complete lysis of fibrin in this region of the clot.

Fibrinolysis with tPA was greatly enhanced when the clot structure contained 2.2 μM glu-plasminogen (equilibrated with the fibrin) prior to the lytic therapy (Fig. 5, *D–F*) when compared to lysis of a clot containing no plasminogen. Permeation had a large enhancing effect on the extent of lysis. For a 5-min bolus of 1 μM tPA, over 0.2 cm of the clot was fully lyzed after 15 min at $\Delta P/L$ = 50 mm-Hg/cm. This is in contrast to mild lysis of less than 0.1 cm of the gel at $\Delta P/L$ = 1 mm-Hg/cm. The concentration profiles for each species after 15 min of lysis for $\Delta P/L$ = 50 mm-Hg/cm are given in Fig. 5, *E* and *F*. Release of bound species from the fully lyzed front of the clot accounts for the increase in the plasminogen and tPA concentration in the free phase at x = 0.2 cm. Continuous infusion of glu-plasminogen into the clot leads to the concentration profile seen in Fig. 5 *E*. Ahead of the lysis front at x = 0.3 cm, significant quantities of bound tPA led to rapid local conversion of bound glu-plasminogen to plasmin. For fibrinolysis *in the absence of the inhibition reactions* (by PAI-1 or antiplasmin), the delivery by permeation of only a few micrograms of active tPA for a few min into a clot was predicted to result in kinetically significant plasminogen activation and fibrinolysis over the course of 15 min.

Plasminogen activation by uPA and lysis under conditions of permeation

Similar to the above analysis, we have conducted simulations of fibrinolysis using a 5-min bolus administration of 1 μM urokinase (uPA). These simulations were run for a coarse compacted clot containing *no* plasminogen prior to lysis (Fig. 6, *A–C*) or equilibrated with plasminogen (Fig. 6, *D–F*) prior to lysis. Fibrinolysis mediated by uPA was greatly enhanced by the presence of permeation driven by a pressure drop of 50 mm-Hg/cm (Fig. 6 *A*) as compared to lysis under a $\Delta P/L$ of 1 or 10 mm-Hg/cm. Since uPA had no ability to bind fibrin, it was able to penetrate deeply into the clot at high pressure drops. With high permeation rates of uPA into the clot, the lysis rate was high in the interior of the clot as well as at the front of the clot. In contrast to the simulations for tPA, the plasmin generated by uPA reached relatively high levels in the free phase (Fig. 6 *B*). Even a highly lyzed region (>80%) of the clot had significant capacity to bind plasminogen (Fig. 6 *C*). When the clot was equilibrated with glu-plasminogen, lysis was particularly intense within the clot interior at x = 0.1 cm where the urokinase had penetrated so as to achieve full lysis within the clot but not at the front of the clot (Fig. 6 *D*). In reality, this would lead to a flow-induced collapse of the clot which we have not modeled since the fibrin was defined as the non-mobile, stationary phase. Where lysis reached 100% locally at x = 0.1 cm, the bound concentrations of the species went to zero as expected (Fig. 6 *F*). At $\Delta P/L$ = 50 mm-Hg/cm, the preexisting free plasminogen is rapidly activated locally where the urokinase bolus has penetrated (Fig. 6 *E*) but plasminogen was replenished behind the bolus with fresh perfusate. The local depletion of plasminogen by urokinase in the fluid phase led to reduced plasminogen binding to the fibrin and enhanced plasmin adsorption to fibrin at this position of the clot (Fig. 6 *F*).

Effects of fibrin fiber radius on lysis

The ionic strength during fibrinogen polymerization controls the thickness of the fibrin fibers. The fibers may be very fine with only a few protofibrils associated together or may be very coarse with hundreds of fibrils in a fiber bundle. To explore the effects of fiber radius on transport and kinetics, we carried out simulations at constant Peclet number (Pe) or constant $\Delta P/L$ for lysis of clots with the same bulk fibrin concentration but with varying initial fiber radius R_{fo} from 25 to 500 nm. The time to achieve 50% average lysis (T_{50}) was used as an index of the overall lytic efficiency.

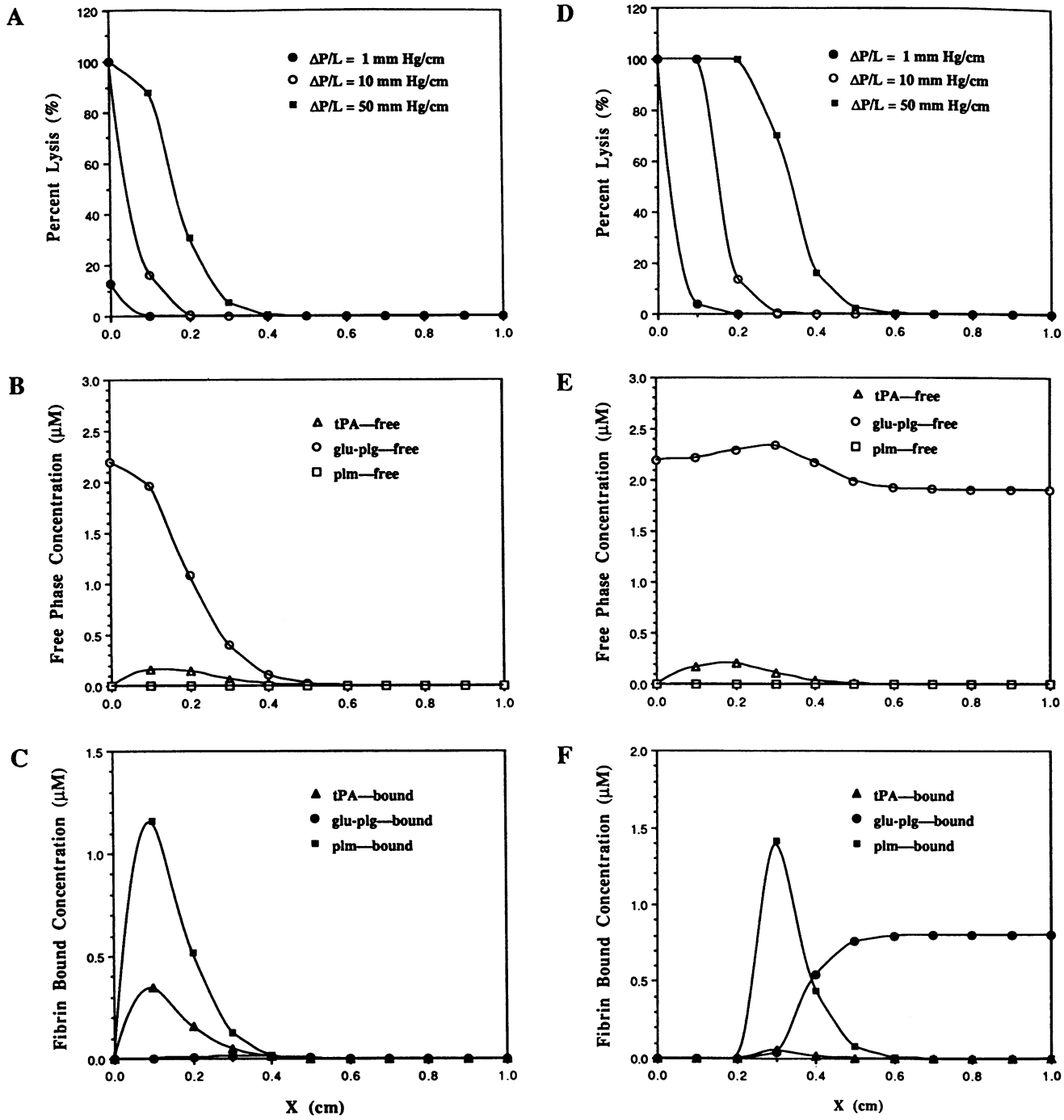

FIGURE 5 Fibrinolysis mediated by tPA of a coarse, compacted clot. Fibrin structure and inlet conditions were identical to those of Fig. 4. Penetration of a lytic front after 15 min was greatly enhanced under conditions of increasing permeation at $\Delta P/L$ = 1, 10, and 50 mm-Hg/cm-clot for lysis of clots that contained no glu-plasminogen before lysis (*A*). The free phase (*B*) and fibrin bound (*C*) concentration profiles for glu-plasminogen, plasmin, and tPA are given for lysis after 15 min at a $\Delta P/L$ = 50 mm-Hg/cm-clot. Lysis after 15 min was greatly enhanced under conditions of increasing permeation as seen at $\Delta P/L$ = 1, 10, and 50 mm-Hg/cm-clot for lysis of clots that contained glu-plasminogen (c^b_{plg} = 0.940 μM and c^f_{plg} = 1.856 μM) prior to the lytic regime (*D*). The free phase (*E*) and fibrin bound (*F*) concentration profiles for glu-plasminogen, plasmin, and tPA are given for lysis after 15 min at a $\Delta P/L$ = 50 mm-Hg/cm-clot.

In simulations at constant pressure drop, fine fibers caused a reduction in specific permeability, while coarse fibers led to enhanced permeation and subsequently enhanced lysis rates and reduced T_{50} (Fig. 7, *A* and *C*). For plasma clots (8.823 μM fibrin), a very slight minimum was seen in the T_{50} for very coarse fibers undergoing lysis at a constant $\Delta P/L$ = 0.01 mm-Hg/cm (Fig. 7 *A*). This was due to the competing effects of reduced permeation and enhanced available site concentration in fine clots; coarse clots had high specific permeability, but reduced available site concentrations (Eq.

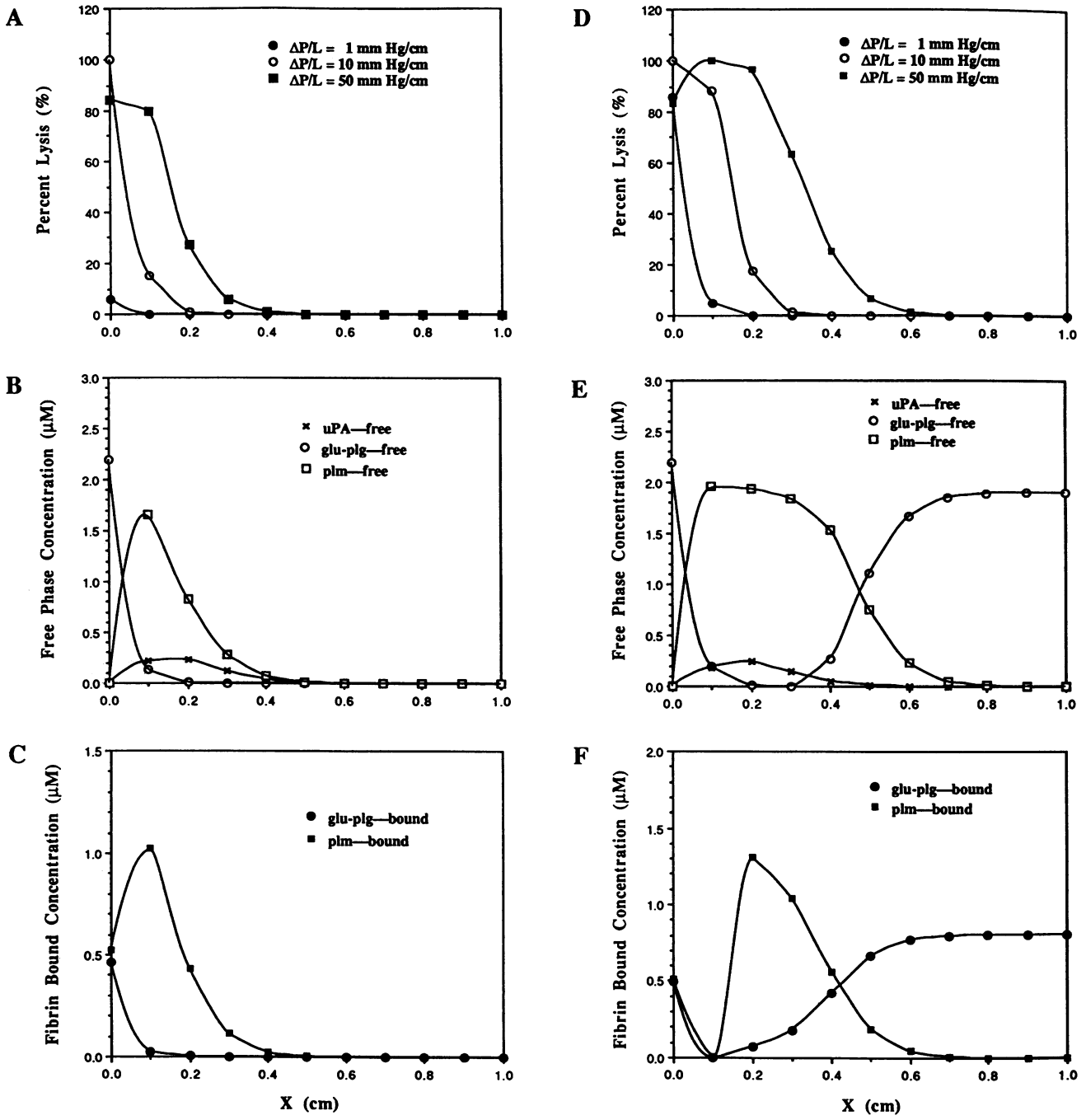

FIGURE 6 Fibrinolysis mediated by urokinase (uPA) of a coarse, compacted clot. Fibrin structure and inlet conditions were identical to those of Fig. 4 except that uPA was used instead of tPA as the lytic agent. Lysis after 15 min was greatly enhanced under conditions of increasing permeation as seen at $\Delta P/L$ = 1, 10, and 50 mm-Hg/cm-clot for lysis of clots that contained no glu-plasminogen before lysis (*A*). The free phase (*B*) and fibrin bound (*C*) concentration profiles for glu-plasminogen, plasmin, and uPA are given for lysis after 15 min at a $\Delta P/L$ = 50 mm-Hg/cm-clot. Lysis after 15 min was greatly enhanced under conditions of increasing permeation as seen at $\Delta P/L$ = 1, 10, and 50 mm-Hg/cm-clot for lysis of clots that contained glu-plasminogen (c^b_{plg} = 0.940 μM and c^f_{plg} = 1.856 μM) before lysis (*D*). The free phase (*E*) and fibrin bound (*F*) concentration profiles for glu-plasminogen, plasmin, and uPA are given for lysis after 15 min at a $\Delta P/L$ = 50 mm-Hg/cm-clot.

6 and 9). At constant $\Delta P/L$ greater than about 0.02 mm-Hg/cm across plasma clots subjected to a 5-min bolus of either 1 μM tPA or uPA, no minimum in the T_{50} profile was seen since the permeability effects became more pronounced and controlled the lysis rates. In general, at $\Delta P/L$ greater than 0.02 mm-Hg/cm, the coarser the plasma clot, the faster it lysed. With compacted clots, coarse fibers led to a greater permeability such that 50% overall lysis was achieve within about 20 min for a bolus of 1 μM of either uPA or tPA (Fig. 7 *C*). Compacted clots with fine fibers had very low specific permeability and required in excess of 100 min to achieve 50% average lysis.

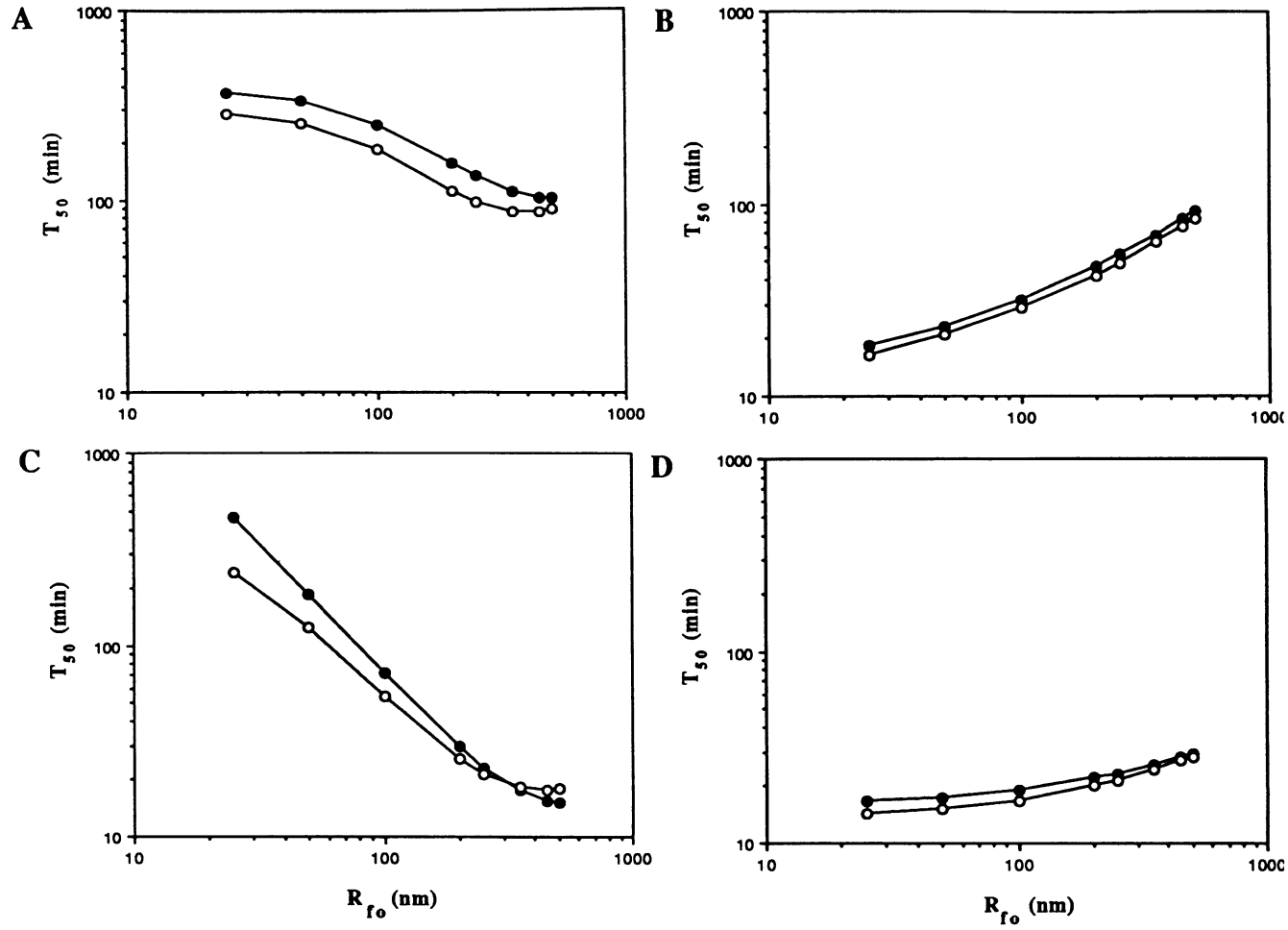

FIGURE 7 Effect of initial fiber radius (R_{fo}) on the time to achieve 50% average lysis (T_{50}). Simulations for lysis of plasma clots (8.8 μM fibrin) (*A, B*) or compacted clots (220 μM fibrin) (*C, D*) were run at a constant pressure drop of 0.01 mm-Hg/cm (*A*) or 50 mm-Hg/cm (*C*) or at constant permeation velocity (constant Pe = 421) (*B, D*). An inlet condition was set for a 5-min bolus of either 1 μM tPA (○) or uPA (●) with continuous introduction of 2.2 μM glu-plasminogen at the inlet. In all cases, fibrin was equilibrated with 2.2 μM glu-plasminogen (c^b_{plg} = 0.940 μM and c^f_{plg} = 1.856 μM) prior to lysis.

Simulations run at constant Pe = 421 (i.e., constant velocity) correct for the fact that gels with fine fibers have a lower specific permeability than gels at the same bulk fibrin density with thick fibers. The pressure drop across the clot was adjusted in order to maintain constant Pe. For plasma clots, the pressure drop was adjusted from 5.25 mm-Hg/cm (R_{fo} = 25 nm) to 0.013 mm-Hg/cm (R_{fo} = 500 nm) to maintain constant Pe (Fig. 7 *B*). For compacted clots, the pressure drop was adjusted from 5000 mm-Hg/cm (R_{fo} = 25 nm) to 12.5 mm-Hg/cm (R_{fo} = 500 nm) to maintain constant Pe (Fig. 7 *D*). Although simulations at constant velocity are feasible numerically, experiments run under these conditions (such as $\Delta P/L$ = 5000 mm-Hg/cm) will cause flow-induced compaction of the lysing fibrin—a front sharpening effect with large dynamic changes in fibrin density. The model, which treats the fibrin as an immobile network, can not account for such effects.

In Fig. 7 B, a 5-min bolus of 1.0 μM uPA or tPA (at perfusion velocity) lyzed fine plasma clots faster than coarse clots. This is expected stoichiometrically since more fibrin monomers are hidden inside the thick fibers while thin fibers have exposed on their outer surface more of the fibrin monomers. Reduction of accessible monomers leads to a reduction of available binding and reaction sites (Eq. 6 and 9). A 20-fold increase of fiber radius (25 nm to 500 nm) caused a prolongation by about 5-fold of the T_{50} of very coarse plasma gels compared to very fine plasma gels. With a lytic regime of a 5-min bolus of 1 μM tPA or uPA and constant Pe = 421, the T_{50} of compacted clots (220 μM fibrin) was only slightly less for fine clots than for coarse clots (Fig. 7 *D*). In the dense compacted clots, a 20-fold increase of fiber radius caused only a modest 1.8-fold increase of T_{50}. This was due to the fact that in dense clots, the available concentration of binding and reaction sites of the fibrin were in great excess and were not strongly limiting relative to the concentrations of plasminogen, tPA, or uPA.

Observations of fine gels (formed in angiographic contrast fluid) being resistant to lytic agents (Carr and Hardin, 1987; Nair et al., 1991; Gabriel et al., 1992) are thus likely due to intrinsic changes in enzyme kinetic constants or adsorption rate constants, and are less likely to be mediated by transport

processes. In vivo, fine clots may be resistant to lytic therapy by two mechanisms: alteration of intrinsic adsorption or reaction kinetics and poor inner clot permeation.

Relaxation of steric hindrance constraint for binding and reaction

In calculating the binding site concentrations on the surface of the fibrin fibers we have assumed that only the protofibrils on the outer surface of the fiber were sterically accessible for adsorption or reaction. Relaxation of this steric hindrance constraint can be achieved simply by including some inner "shells" of protofibrils in addition to the outer shell of protofibrils (see Appendix). The number n of protofibril "shells" available for reaction is related to a multiplying factor κ by $n = (\kappa + 1)/2$. For $\kappa = 1$, only the outer "shell" of protofibrils of the fiber participated in reactions, while for $\kappa = R_f/r_o$ all the monomers in the protofibrils of the fiber were available. Setting $\kappa = R_f/r_o$ is equivalent to having the bulk concentration of fibrin available for all reaction and adsorption processes. By increasing the volume-averaged site concentration θ_i with increasing κ, the adsorption rates of tPA, plasminogen, and plasmin are enhanced with subsequent enhancement of plasminogen activation, plasmin binding, and fibrin degradation. Relaxation of the steric hindrance constraint to allow for protofibrils within the deeper interior of the fiber to participate in reactions led to an expected kinetic enhancement of the lysis rate (Fig. 8). In clots of low fibrin concentration (8.823 μM), the sites for adsorption and reaction are limiting (relative to the concentration of the 5 min bolus) and fibrinolysis was enhanced by including more protofibrils of the fiber with increasing κ (Fig. 8 *A*). Inclusion

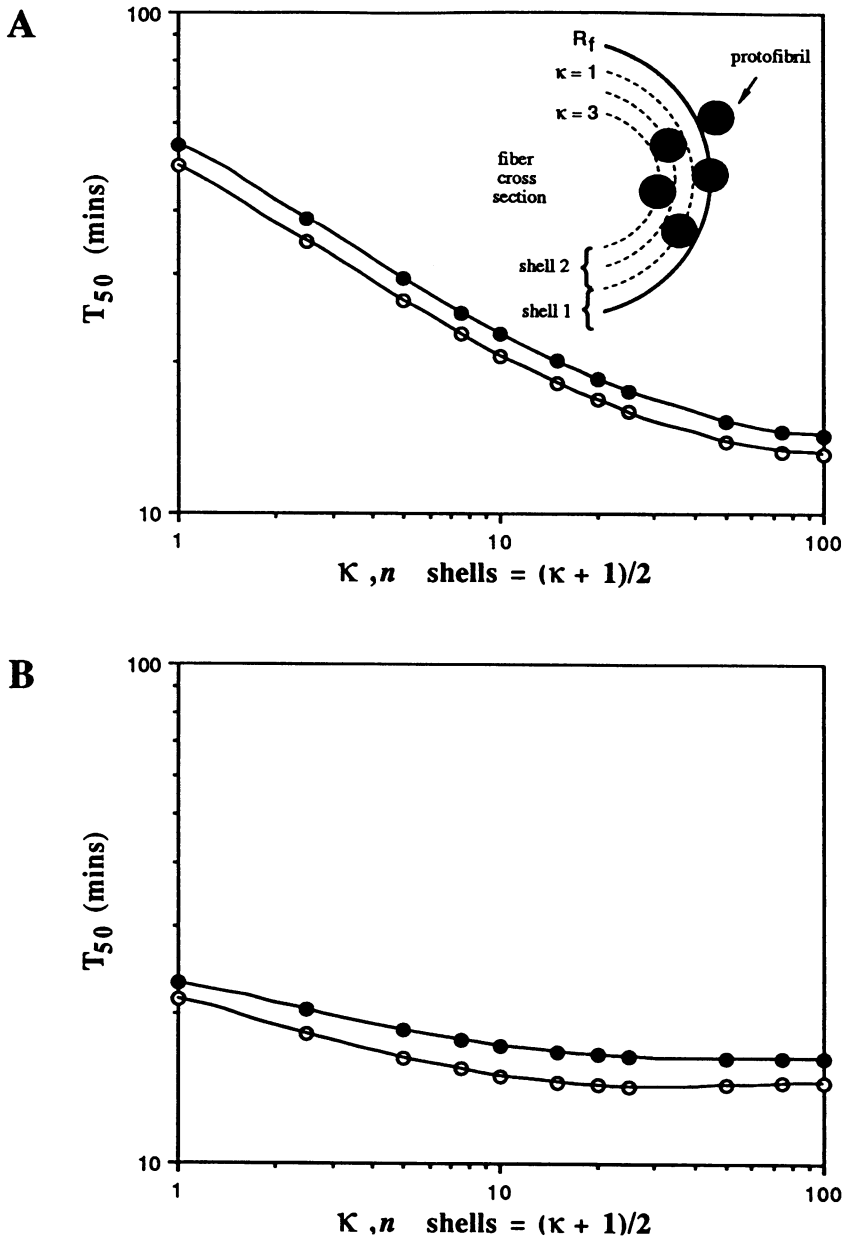

FIGURE 8 Effect of relaxation of steric hindrance constraint on the time to achieve 50% average lysis (T_{50}). Coarse plasma clots (R_{fo} = 250 nm; 8.8 μM fibrin) (*A*) or coarse, compacted clots (R_{fo} = 250 nm, 220 μM fibrin) (*B*) were subjected to a lytic regime of 1 μM uPA (○) or tPA (●) for 5 min with continuous infusion of 2.2 μM glu-plasminogen. The pressure drop was 0.052 (*A*) and 50 mm-Hg/cm (*B*) such that the initial Peclet number was 421 in all cases. The parameter κ is defined in the text and Appendix as an index of the number of protofibril "shells" of the fibrin fiber which can participate in adsorption and reaction during fibrinolysis (See insert). The number of shells n is defined as $(\kappa + 1)/2$. For $\kappa = 1$ only the outer shell of fibrils participate in adsorption and reaction, while for $\kappa = 100$ nearly all the fibrils in the fiber were available for adsorption or reaction.

of just two outer "shells" of protofibrils of the fiber ($\kappa = 3$) led to a sufficiently high site concentration in compacted clots such that plasminogen activation and plasmin activity were not limited by the number of fibrin sites. In these dense clots, increasing κ greater than 1 had little effect on T_{50} suggesting that the steric hindrance constraint is not a significant limitation for lysis of these clots. During fibrinolysis of real fibrin, the fibers may swell or fray as lysis proceeds such that more protofibrils participate in the reactions (equivalent to κ increasing). Such a phenomena would likely depend on the extent of crosslinking. From Fig. 8, it appears that the enhancement in lytic rates due to this swelling of the fibers would be relatively minor for dense clots but several fold for plasma clots.

Comparison of Glu versus Lys plasminogen

Although we have not considered the enzymatic conversion of glu-plasminogen to lys-plasminogen or the generation of lys-plasmin, it was possible to run the model using binding and reaction constants for lys-plasminogen (Tables 1 and 2). Lys-plasminogen is activated more rapidly than glu-plasminogen by either uPA or tPA. Additionally, lys-plasminogen binds fibrin with much greater avidity than glu-plasminogen. Simulations of lysis demonstrated that lys-plasminogen was much more effective than glu-plasminogen in facilitating fibrinolysis of either plasma clots or flow-compacted clots (Fig. 9). Under the conditions tested, the reduced mobility and strong fibrin partitioning of lys-plasminogen did not significantly reduce its capacity to be activated by urokinase. In contrast, the stronger avidity between uPA and free phase lys-plasminogen led to rapid activation to form lys-plasmin. Although lys-plasminogen led to more rapid lysis when compared to glu-plasminogen under conditions of flow, the extent of this enhancement was dependent on the initial conditions and time of simulation. Lys-plasmin may have some advantage in that it is more rapidly formed on fibrin by tPA, thus protecting it from antiplasmin inhibition.

How important is permeation?

Permeation of fibrinolytic mediators through the interstitial regions of a blood clot is expected if a pressure drop exists

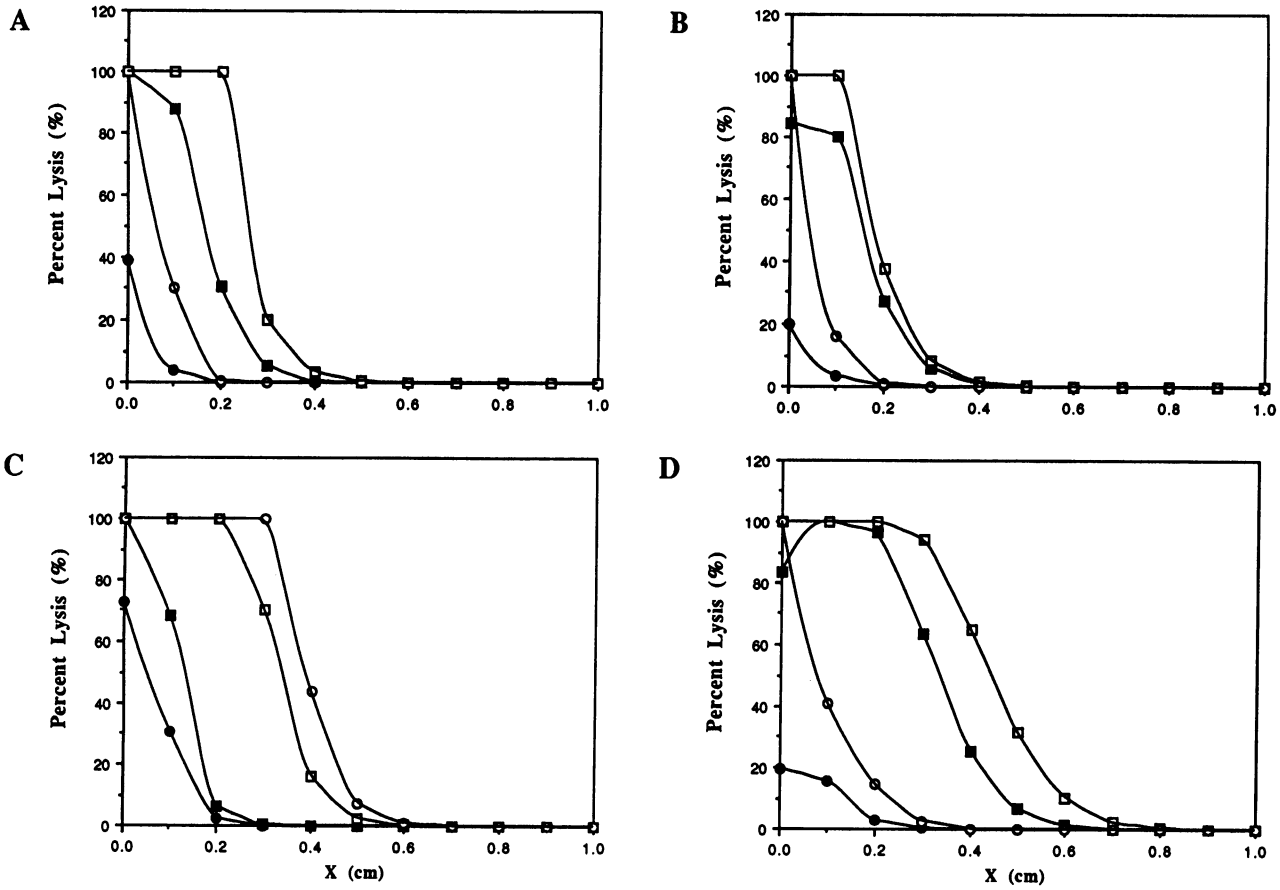

FIGURE 9 Effect of glu-plasminogen and lys-plasminogen on the spatial distribution of lysis after various times. Lysis profiles are given after 5 min (*circles*) and 15 min (*squares*) for lysis with glu-plasminogen (*solid symbol*) or lys-plasminogen (*open symbol*). Simulations were for the lysis at $\Delta P/L = 0.052$ mm-Hg/cm of a coarse, plasma clot subjected to a 5-min bolus of 1 μM tPA (*A*) or uPA (*B*) or for the lysis at $\Delta P/L = 50$ mm-Hg/cm of a coarse, compacted clot subjected to a 5-min bolus of 1 μM tPA (*C*) or uPA (*D*). In all simulations, the clots were prelaid and equilibrated with 2.2 μM of the plasminogen subtype indicated.

across the clot. Although no measurement of this interstitial fluid velocity within real blood clots has ever been made, the ability to reperfuse an arterial thrombi within an hour after initiation of thrombolytic therapy strongly suggests that diffusion is not the sole mode of transport. To demonstrate the very strong impact of permeation processes on thrombolytic therapy, we have run simulations over a wide range of transport regimes ranging from diffusion dominated (Pe < 1) to convection dominated (Pe > 1). The transition between these regimes is seen for lysis of plasma clots (Fig. 10 *A*) and flow-compacted clots (Fig. 10 *B*). Without permeation, a coarse compacted clot exposed to 1 μM tPA for 5 min will require over 1000 min to achieve 50% lysis. With fluid permeation, this same lytic regime of 5-min bolus of 1 μM tPA required under 20 min. Moving from a strongly diffusion-controlled regime to a strongly convection-controlled regime leads to an 98% reduction in T_{50}. In our own measurements of lysis fronts moving across fine fibrin gels (8.8 μM fibrin) (S. Diamond and J.H. Wu, unpublished observation), we have observed about a 10-fold increase of lysis with the addition of a pressure drop of 3.5 mm-Hg/cm-clot to push a 1 μM plasmin solution through the gel (see Discussion).

Role of administration regime on lysis

We have calculated the effect of using tPA and/or uPA at various concentrations under bolus and continuous administration regimes. Clinically, thrombolytic therapy is initiated with a bolus dose followed by a low level infusion (*Physicians' Desk Reference*, 1992). These administration regimes can be simulated by changing the inlet concentration of each

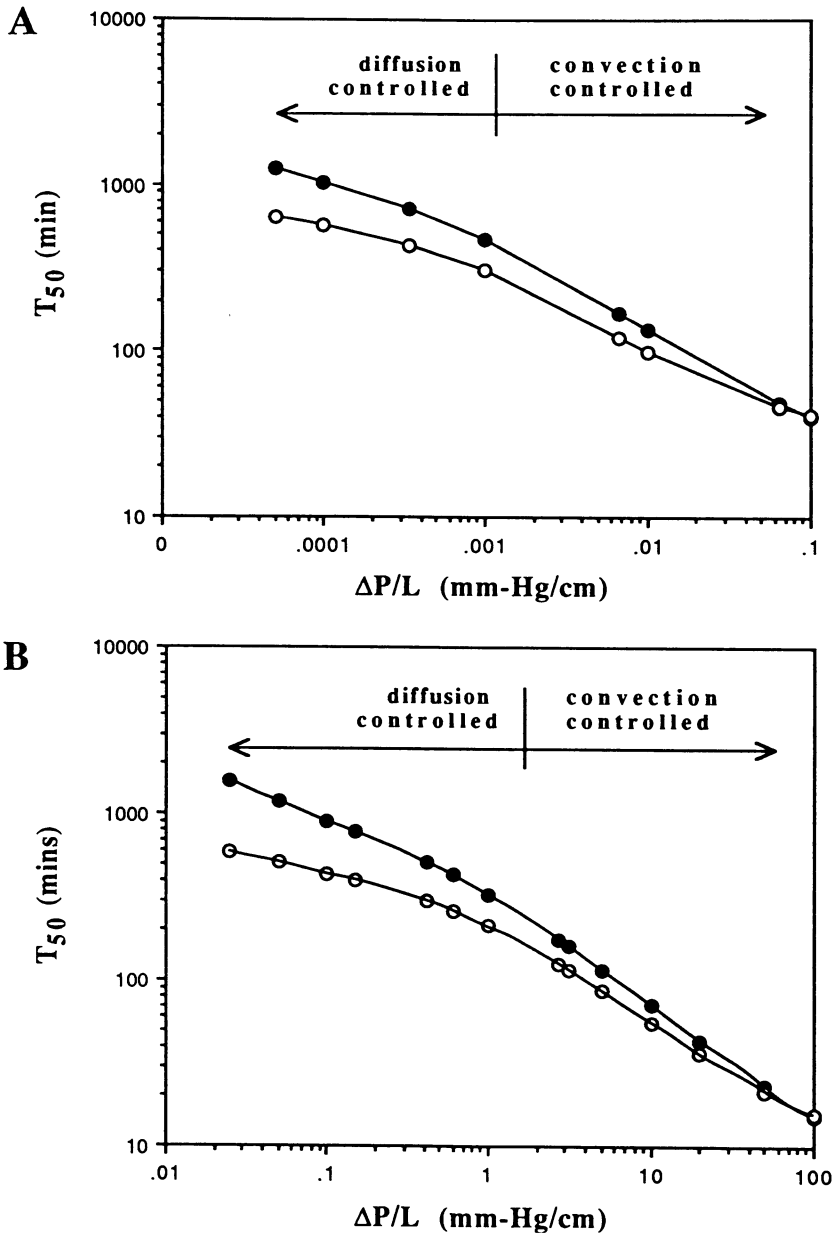

FIGURE 10 The effect of pressure drop on the time to achieve 50% average lysis (T_{50}) for lysis of coarse plasma clots (*A*) or coarse compacted clots (*B*). The lytic regime was a 5-min bolus of either 1 μM uPA (○) or tPA (●) with continuous infusion of 2.2 μM glu-plasminogen.

species (Eq. 17a) to accommodate multiple bolus or other infusion strategies. In Table 4, the time needed to achieve 50% average lysis (T_{50}) is given as an index of the efficiency of the administration regime.

In Table 4, the delivery of 1 μM tPA for 5 min (4.5 μg tPA delivered into the clot) was sufficient to lyze half the clot within 23 min. Doses of tPA sustained for 10 and 20 min or higher concentrations of tPA (5 μM) reduced T_{50} only slightly compared to the 5 min bolus of 1 μM tPA. Similarly for uPA, increases beyond a 5 minute bolus of 1 μM uPA provided for only minor reductions of the T_{50}. Under permeation conditions, even very low levels (0.1 μM) of uPA or tPA provided for kinetically significant lysis. This occurred since inhibition of tPA, uPA, or plasmin was not considered. Delivery of plasmin directly into a clot structure however was not a particularly efficient lytic approach compared to the equivalent delivery of uPA or tPA. Plasmin was predicted to penetrate poorly through the clot due to its strong binding. Also, plasmin can not continually activate plasminogen within the clot. No large advantage was gained using multiple bolus infusions or a bolus followed by continuous infusion; however, these results are influenced by the absence of the inhibition reactions which would serve to consume tPA or uPA. In general, under permeation conditions in the absence of inhibition reactions, the first plasminogen activator to reach the clot in the first minutes will contribute the most to the overall lysis. Subsequent amounts of lytic agent which penetrate the clot at later times have a lesser impact on the overall fibrinolysis.

Designing thrombolytic agents

With a numerical model of fibrinolysis, it was possible to evaluate the outcomes which may occur by creating a new fibrinolytic mediator using protein engineering. Several chimeric molecules have been developed and new wildtype plasminogen activators are occasionally discovered (for example, bat-tPA). By numerically modulating the fibrin affinity or reaction kinetics of a fibrinolytic mediator and evaluating the therapeutic advantage, some guidelines for protein engineering may emerge. Although the specific permeability of a clot controls lysis to a large extent, gains are possible through protein engineering a plasminogen activator or fibrinolytic mediator. These simulations do not take into account the role of the inhibition reactions.

By numerically adjusting the adsorption rate constant (k_f) for tPA to fibrin while keeping the desorption rate constant (k_r) fixed, it was possible to evaluate the effects of changing the K_d of tPA for fibrin. Increasing the K_d of tPA for fibrin by reducing the k_f from the wildtype value of 1.148×10^{-4} $\mu M^{-1} s^{-1}$ to 5×10^{-8} $\mu M^{-1} s^{-1}$ resulted in a strong reduction in lytic efficacy. This change in k_f led to a prolongation of the T_{50} from 25 min to nearly 1000 min for a 5-min bolus of tPA (1 μM) administered ($\Delta P/L$ = 50 mm-Hg/cm) to a coarse, compacted clot prelaid with plasminogen. Interestingly, reducing the K_d of tPA for fibrin by increasing the k_f from 1.148×10^{-4} $\mu M^{-1} s^{-1}$ to 10^{-1} $\mu M^{-1} s^{-1}$ also resulted in a reduction in lytic efficacy by a factor of two as indicated in a prolongation of the T_{50}. It was also possible to modulate the K_d of tPA for fibrin by adjusting the desorption rate constant k_r while keeping k_f fixed. Using this approach, there was no change in T_{50} as a result of reducing the K_d from its wildtype value of 0.58 μM to 0.1 nM for lysis of a coarse compacted clots prelaid with plasminogen. Increasing the K_d of tPA for fibrin from 0.58 μM to 100 μM caused only a 15% prolongation of the T_{50}.

This type of analysis would suggest that the efficacy of tPA under flow conditions is nearly optimal for wildtype tPA or recombinant tPA value of K_d = 0.5 μM. By increasing the K_d slightly, tPA can penetrate into a clot structure somewhat more easily, however, this advantage in clot penetration is offset by poor activation of fibrin bound plasminogen. Interestingly, there was a disadvantage in reducing the K_d of tPA for fibrin into the nM range by increasing k_f. Under flow conditions, increasing the forward adsorption rate constant reduces the ability of tPA to penetrate into the clot with consequent reduction in lytic efficiency. In general, when tPA comes off the fibrin faster than bound plasminogen, the kinetic rate of lysis is reduced.

By numerically increasing the adsorption rate constant k_f of plasminogen to fibrin from the wildtype value of 1.087×10^{-4} $\mu M^{-1} s^{-1}$ to 10^{-1} $\mu M^{-1} s^{-1}$ provided no advantage in lytic efficiency (as indicated by the T_{50}) for lysis of coarse compacted clots with tPA under flow conditions. This is expected since tPA and plasminogen adsorb at roughly the same rates. However reducing the adsorption rate constant k_f of plasminogen to fibrin from the wildtype value of 1.087×10^{-4} $\mu M^{-1} s^{-1}$ to 10^{-9} $\mu M^{-1} s^{-1}$ led to a 6-fold increase in the T_{50}. This indicated that sufficiently rapid adsorption of plasminogen to fibrin was a critical step for tPA-mediated plasminogen activation to proceed in a kinetically efficient manner. It was also possible to modulate the K_d of plasminogen for fibrin by adjusting the desorption rate constant k_r while keeping k_f fixed. Using this approach, there was no change in T_{50} as a result of reducing the K_d from its wildtype value of 38 μM to 0.1 nM for lysis of a coarse compacted clots prelaid with plasminogen. Increasing the K_d from 38 μM to 1000 μM caused only a modest 30% prolongation of the T_{50}.

It was found that increasing the K_d of plasmin to fibrin by increasing the rate of desorption (keeping k_f fixed) led to a decrease in the rate of lysis and a consequent increase in the time required to achieve T_{50}. Increasing the K_d from the nM range to 100 μM served to prolong T_{50} by a factor of about 1.5 for both tPA and uPA-mediated lysis. The rate of lysis has been modeled to depend on the bound plasmin concentration and therfore it is reasonable to expect that increasing the rate of desorption reduces the amount of fibrin solubilized.

When the K_d of plasmin was altered by keeping the rate of desorption constant and increasing the rate of adsorption, no effect was observed for tPA-mediated lysis. However, it was found that for uPA-mediated lysis, increasing the rate of adsorption from 10^{-7} $\mu M^{-1} s^{-1}$ to 0.05 $\mu M^{-1} s^{-1}$ led to a

TABLE 4 Comparison of administration regimes

Infusion scheme	Time to achieve 50% overall lysis (min)
Bolus delivery	
5 min B (0.1 μM tPA)	33.43
5 min B (1.0 μM tPA)	23.03
5 min B (5 μM tPA)	18.33
10 min B (1.0 μM tPA)	22.33
20 min B (1.0 μM tPA)	22.27
5 min B (0.1 μM uPA)	28.6
5 min B (1.0 μM uPA)	21.4
5 min B (5.0 μM uPA)	18.3
10 min B (1.0 μM uPA)	21.17
20 min B (1.0 μM uPA)	21.17
5 min B (0.1 μM plm)	>1500*
5 min B (1.0 μM plm)	111.0
5 min B (2.2 μM plm)	67.1
E (1.0 μM tPA; $\tau_{1/2}$ = 5 min)	23.4
E (1.0 μM uPA; $\tau_{1/2}$ = 5 min)	21.7
E (1.0 μM tPA; $\tau_{1/2}$ = 15 min)	22.7
E (1.0 μM uPA; $\tau_{1/2}$ = 15 min)	21.4
Continuous infusion	
C (0.1 μM tPA + 0.1 μM uPA)	25.5
C (0.1 μM tPA + 1.0 μM uPA)	20.8
C (1.0 μM tPA + 0.1 μM uPA)	21.9
C (1.0 μM tPA + 1.0 μM uPA)	19.4
C (5.0 μM tPA + 0.1 μM uPA)	18.2
C (0.1 μM tPA + 5.0 μM uPA)	18.1
Bolus + continuous infusion	
5 min B (1.0 μM tPA) + C (0.1 μM tPA)	22.9
5 min B (1.0 μM tPA) + C (0.1 μM uPA)	22.3
5 min B (1.0 μM uPA) + C (0.1 μM tPA)	20.9
5 min B (1.0 μM uPA) + C (0.1 μM uPA)	21.3
5 min B (5.0 μM tPA) + C (0.1 μM uPA)	28.5
5 min B (5.0 μM uPA) + C (0.1 μM tPA)	18.1
Double bolus infusion	
5 min B (1.0 μM tPA) + 5 min wait + 5 min B (1.0 μM tPA)	22.9
5 min B (1.0 μM tPA) + 10 min wait + 5 min B (1.0 μM tPA)	23.0
5 min B (1.0 μM uPA) + 5 min wait + 5 min (1.0 μM uPA)	21.3
5 min B (1.0 μM uPA) + 10 min wait + 5 min B (1.0 μM uPA)	21.4
5 min B (1.0 μM tPA) + 5 min wait + 5 min B (1.0 μM uPA)	22.9
5 min B (1.0 μM tPA) + 10 min wait + 5 min B (1.0 μM uPA)	23.1
5 min B (1.0 μM uPA) + 5 min wait + 5 min B (1.0 μM tPA)	21.2
5 min B (1.0 μM uPA) + 10 min wait + 5 min B (1.0 μM tPA)	21.3

* 1666 min to achieve 42.7% lysis.

The time needed to achieve 50% overall clot lysis is predicted for various administration regimes with 2.2 μM glu-plg in the permeating fluid (B = Bolus; C = Constant continuous infusion; E = Exponential decay given by $C_o \cdot \exp(-t/\tau_{1/2})$, where $\tau_{1/2}$ is the half-life of the agent at the clot inlet). Simulations were for lysis of a flow-compacted (220 μM fibrin), coarse (R_{fo} = 250 nm) clot, equilibrated with 2.2 μM glu-plg (c^b_{plg} = 0.940 μM; c^f_{plg} = 1.856 μM) prior to lysis. The permeation was driven by $\Delta P/L$ = 50 mm-Hg/cm in all simulations (initial Pe = 421 and permeation velocity = 2.10×10^{-4} cm/s).

5-fold decrease in T_{50}. It has beeen pointed out earlier (Fig. 6 *E*) that the fluid phase concentration of plasmin reaches high levels for lysis with 1 μM uPA. Consequently, increasing the rate of adsorption leads to higher levels of bound plasmin and therefore higher lysis reates. For tPA-mediated lysis, the plasmin tends to remain bound to fibrin and therefore alteration of the rate of adsorption does not affect the rate of lysis in any significant way.

In other simulations, increasing the k_2 of the plasminogen activation reaction by either tPA or uPA led to more rapid lysis. For example, increasing the k_2 of plasminogen activation by tPA from the wildtype value of 0.1 s^{-1} to 100 s^{-1} reduced the T_{50} by half. The gains were similar to the gains seen by increasing the dose of tPA or uPA delivered into a clot. Reducing the K_m of tPA for bound plasminogen from the wildtype value of 0.16 μM to 0.1 nM had no effect on lytic efficiency.

DISCUSSION

Considerable debate still exists on what properties the ideal plasminogen activator should have (Haber, 1989). Some workers believe strong binding of fibrin is essential. Fibrin specificity is considered the main advantage of tPA, potentially leading to clot-specific dissolving power. However, significant reduction of circulating fibrinogen levels is found in patients treated with recombinant tPA, indicating systemic plasminogen activation. Fibrinogenolysis also can occur with the use of urokinase and streptokinase which lack the ability to bind fibrin. Other workers contend that a cocktail of prourokinase and tPA is most effective. The advent of thrombolytic therapy has driven the development of second and third generation recombinant plasminogen activators. Prediction of clinical efficacy using animal models or in vitro data is still difficult, and optimization of thrombolytic therapy requires human clinical studies. From our numerical calculations of fibrinolysis, we predict that

1. Penetration of tPA or uPA into a clot structure by pressure-driven permeation must occur during thrombolytic therapy, and is the dominant mode of transport. If diffusion were the only mechanism of transport, lysis would require many hours or days to occur. The penetration rate of the lytic agent is a major regulator of the time needed to dissolve a clot.

2. The penetration of tPA into the clot is slowed by its strong binding to the fibrin. The transport of tPA (as well as lys-plasminogen and plasmin) as it moves through a clot is not at local equilibrium since adsorption is relatively fast and strong while desorption is slow.

3. In agreement with many experimental investigations, the prevailing concentration of plasminogen prebound to the clot or perfused into the clot has a strong impact on the lysis rates. The use of tPA and uPA together may also be advantageous due to transport phenomena where uPA provides for a leading wave of lysis moving with the permeation front, while tPA leads to strong lysis of the front of the clot.

4. The long clots of the venous system have a relatively low ΔP/L across them which may make them resistant to thrombolytic therapy. Improvement of lytic therapies for these clots should focus on improvement of transport processes. Long clots extending the length of a large vessel

would most likely benefit from reduced fibrin binding of the plasminogen activator. In short clots of less than a centimeter in length, fibrin binding capacity may be beneficial and penetration distances short enough, to advocate tPA usage.

The measurement of plasminogen activation rates and clot solubilization rates on whole clots when conducted without permeation may lead to apparent kinetic constants which may be at least an order of magnitude too slow due to diffusion limits. To avoid these transport limitations, the measurement of intrinsic kinetics of fibrinolysis requires mechanically-dispersed fibrin, gradientless reactions in well mixed systems, or very small diffusion lengths such as those found in fibrin films. Diffusion limits may exist in experiments which use preformed fibrin clots exposed to a bulk solution of a lytic cocktail, even if that cocktail is well mixed outside the clot. With pressure driven permeation, the full potential of the lytic agents as well as other phenomena can be studied as they likely exist in vivo.

From these simulations, some generalizations can be made about the protein engineering of agents for arterial thrombolytic therapy. First, ultrahigh fibrin affinity uPA-IgG chimerics (K_d < 100 nm) may prove less useful in vivo due to poor clot penetration. This limitation of a uPA-IgG chimeric would not necessarily be observed in vitro unless experiments with permeation were conducted. Chimerics such as uPA active site plus kringle 1 and 2 of tPA may prove useful for targeting uPA to a clot without excessively hindering its ability to penetrate into the clot. There is no gain in enhancing or reducing the fibrin binding avidity of tPA for use of the agent under conditions of permeation.

Earlier modeling work by Zidansek and Blinc (1991) treated uPA-mediated lysis of fibrin as a homogeneous problem with no distinction between species in the fluid phase or in the fibrin phase. This approach is not suitable for tPA-mediated lysis which is distinctly heterogeneous. Additionally, the important effects of plasminogen binding to the clot can not be taken into account with a homogeneous approach. We have made an effort to describe quantitatively the: (i) time evolving fibrin fiber and fibrin density, (ii) adsorption and desorption phenomena under nonequilibrium conditions, (iii) pressure-induced permeation, and (iv) the kinetics of each individual reaction. These important aspects have not been considered in the analysis of Zidansek and Blinc (1991). To our knowledge, this is the first model to account for these four qualitatively and quantitatively important phenomena in fibrinolysis. The earlier modeling efforts of Sobel et al. (1984) and Tiefenbrunn et al. (1986) predict the pharmacodynamics of fibrinolytic mediators in the circulation but make no prediction of actual clot lysis as a function of clot structure or clot composition. The predictions from their model would serve as the initial and boundary conditions for our system of equations.

Very little data exists in the literature where inner clot permeation is controlled or measured during thrombolysis. In work by Blinc et al. (1991), it was reported that a pressure of 27 mm-Hg led to rapid collapse of a fibrin gel during lysis. This high pressure (we estimate the Peclet number to be about 10,000 to 20,000) led to flow-induced collapse of the gel. Flow-induced collapse of a fibrin network is a macroscopic observation of a micro-rheological phenomena which is nearly impossible to quantitatively relate to the actual kinetic events of fibrinolysis. In our in vitro measurements of fibrin gels exposed to pure plasmin at $\Delta P/L$ = 3.5 mm-Hg/cm-clot, we have observed that a lysis front can proceed in a stable fashion for several hours without collapse of the gel structure. This preliminary experimental observation is consistent with our predictions of a stable albeit steep lysis profile which moves forward with time (as seen in Fig. 4). In comparisons of the model to experiments for lysis of fine and coarse gels with continuous infusion of 1 μM plasmin, we have found our simulation to consistently over predict the lysis rate (Fig. 11) even when lysis was constrained to the surface of the fiber (i.e., κ = 1). This may be due to our use of enzyme rates for plasmin cleavage of chromogenic substrates (as compared to the more complex fibrin substrate). In these perfusion experiments with high plasmin concentrations, fine and coarse gels were found to lyze at similar rates. Given the large number of kinetic constants and the uncertainty of certain parameters in our model, validation and improvement of the present model will require many

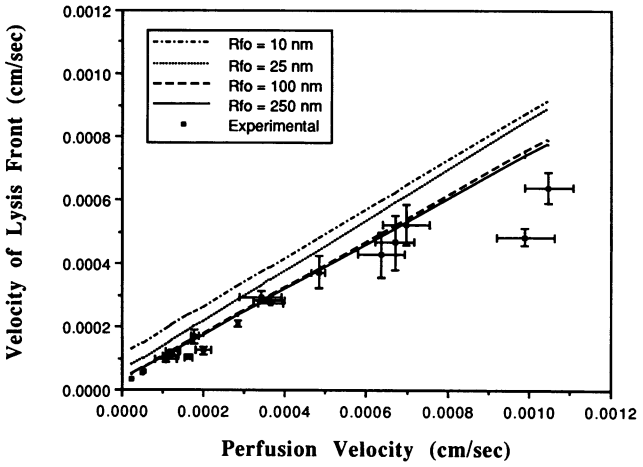

FIGURE 11 Comparison of model predictions with experiments for lysis of non-cross-linked fine and coarse fibrin gels subjected to continuous infusion of 1 μM plasmin. Fibrin gels of 2 cm length were polymerized [3.0 mg/ml fibrinogen (Kabi) with 1 U/ml thrombin (Sigma) for 24 h at 2.5 mM $CaCl_2$ and 0.1 (fine gels) or 0.3 M NaCl (coarse gels)] and then lyzed with plasmin (Sigma) according to the methods of Carr and Hardin (1987) using constant pressure drops from 0.369 to 3.69 mm-Hg/cm-clot. The precise position of the lysis front of each gel was observed microscopically at various time intervals (for calculation of the pseudo steady-state velocity of the lysis front) while the perfusion velocity was measured. The experimentally determined perfusion velocity served as an input into the simulation (as opposed to the pressure drop since several data points were derived from a single experiment). The position of 50% lysis was used as the marker of the lysis front in the simulations. Coarse gels had fibers which were just visible by contrast-enhanced DIC microscopy suggesting that the initial fiber radius was between 100 and 250 nm. Nominal values for the initial fiber radius (R_{fo}) for fine gels were set at 10 and 25 nm in the simulations.

experiments. At this point, we propose that fibrinolysis can be described quantitatively using a convection/diffusion/reaction model. Such a model will be useful in optimizing thrombolytic therapies and in interpreting experimental data to identify molecular mechanisms and test hypotheses.

In future work, the inhibition reactions of PAI-1 and α_2-antiplasmin will be included without major modification of the model. The biochemical role of binding sites on platelet surfaces can be treated by uniformly distributing the sites (with associated K_d's) over the fibrin phase. However, platelets and RBC play a role in the hydrodynamics of the clot by reducing the void volume of the clot available for permeation and by altering the fiber structure. Certainly more complex biochemical and kinetic scenarios for plasminogen activation can be incorporated into the governing transport equations. In clots with multiple layers, it is possible that channeling through paths of least resistance leads to some clinical advantage. Simulation of reperfusion achieved by cannulation of a clot would require solution of the transient, two dimensional (radial and axial) problem which would require accurate prediction of the velocity profile near the wall.

At present the model has no adjustable parameters and uses a single phenomenological parameter (γ) estimated from experiment. The kinetic parameters were evaluated from data obtained with purified systems of mechanically dispersed fibrin. This choice was made in order to avoid analyzing binding data obtained with fibrin gels which may contain diffusional artifacts. Few direct measurements have been made to evaluate the forward and reverse rate constants for different species adsorbing to fibrin in the absence of diffusion limitations. Also, plasminogen activation kinetics are well studied, however very little data are available for intrinsic rate constants of plasmin cleavage of real fibrin cleavage sites. The formulation of the cleavage rate (Eq. 10) as well as the solubilization rate (Eq. 12) was approximate, but does contain the important feature that the rate is proportional to the bound plasmin concentration and the volume-averaged available site concentration. The kinetics of fibrin solubilization by plasmin are not well studied due to the complexity of the phenomena, and are likely modulated by fiber structure and extent of fiber crosslinking.

Currently, the theoretical and experimental basis for quantitatively predicting either hindered diffusion or flow-enhanced dispersion of species which adsorb and react with aperiodic random fibrous media is not complete. In this sense, our formulation of these contributions in Eqs. 3 and 4 has some limitations. However, greater gains in understanding the role of transport processes in fibrinolysis are likely to be achieved through a more accurate knowledge of the specific permeability of real clots since arterial thrombolysis is a convection-dominated problem with a moderate to high Peclet number. Also, direct measurements of the specific permeability and histology/biochemistry of real blood clots formed in the arterial and venous system or formed under controlled in vitro flow conditions will advance the quantitative understanding and predictive optimization of fibrinolysis and thrombolytic therapy.

APPENDIX

In order to quantify the number of binding sites accessible on the fiber surfaces within a given region of the fibrin clot, the total length of fibers initially in the clot was evaluated. Since fibrin fibers have a relatively uniform radius R_f, the total length of fibers is related to the fiber density (ρ_{fiber}), the clot density (ρ_{clot} = gr-fibrin/Vol_T) and the clot total volume, Vol_T (cm^3). The total length of fibers in the gel is given as

$$L_T = (\rho_{clot}) \cdot \frac{(10^{21}\ \text{nm}^3/\text{cm}^3)}{\rho_{fiber}(\pi R_{fo}^2)} \cdot (\text{Vol}_T) \quad \text{for} \quad L_T \quad \text{and} \quad R_{fo}[=]\,\text{nm}.$$

If lysis proceeds from the outside of the fiber inward, the total length of fibrin fibers in the gel is constant with time (Fig. 1). The length of fiber within a volume element $\Delta V = A\Delta x$ is given as

$$L_{\Delta V} = \frac{\Delta x}{\text{L-clot}}(L_T).$$

Since the total clot volume is Vol_T = A·L-clot, the length of fiber per unit volume (nm/cm^3) is

$$\frac{L_{\Delta V}}{\Delta V} = \frac{L_T}{\text{Vol}_T}$$

To evaluate the binding sites on the outer surface of each fiber, it was necessary to know the number of protofibrils on the outer surface of each fiber. The total number of protofibrils N contained in a fiber bundle of R_f can be calculated from the fiber density (Carr and Hermans, 1978) as follows:

$$\rho_{fiber} = 0.28\,\frac{\text{gr-fibrin}}{\text{ml-fiber}}$$

$$\rho_{fiber} = \frac{(\text{MW}_{fbn}/\text{N}_{av})N(2\ \text{monomer}/45\ \text{nm})(\text{L-fibril})}{\pi R_f^2(10^{-21}\text{cm}^3/\text{nm}^3)(\text{L-fiber})}$$

Since L-fibril is equal to L-fiber for fibrils oriented in the direction of the fiber, the number of protofibrils in a fiber is given as

$$N = (0.035061)R_f^2 \quad \text{for} \quad R_f[=]\text{nm}$$

and the protofibril density $p_o = N/(\pi R_f^2)$ in the fiber is

$$p_o = 0.01116\ \text{fibrils/nm}^2 \text{ of fiber cross-sectional area.}$$

According to Carr and Hermans (1978) the volume of water in the fiber is five times the volume of the fibrin in the fiber. Thus, the porosity of the fiber ϵ_{fiber} is 0.8. The fiber porosity is a volume ratio corresponding to

$$\epsilon_{fiber} = 1 - (\text{fibril volume/fiber volume}) = 1 - N(\pi r_o^2)/(\pi R_f^2) = 0.8$$

Thus, an estimate of the protofibril radius excluding all water is calculated (by substitution of p_o into the above equation) to be 2.390 nm which is exactly consistent with the molecular volume of a fibrinogen molecule (density of fibrinogen is 1.39 gr/cm^3). The number of fibrils on the outside of a fiber of radius R_f is defined as the number fibrils which reside on the outer radius of the fiber within one protofibril radius:

$$m(R_f) = \int_0^{2\pi}\int_{R_f - r_o}^{R_f + r_o} p_o r\, dr\, d\theta = [4\pi p_o r_o]R_f$$

For relaxation of the steric hindrance constraint, the number of protofibils which reside within $\kappa \cdot r_o$ of the outer radius R_f of the fiber can be expressed as

$$m(R_f) = \int_0^{2\pi}\int_{R_f - \kappa r_o}^{R_f + r_o} p_o r\, dr\, d\theta = \pi p_o[2R_f r_o(1 + \kappa) + r_o^2(1 - \kappa^2)]$$

This is equivalent to n shells of protofibril which participate in fibrinolysis where $n = (\kappa + 1)/2$. To evaluate the local fiber radius $R_f(x', t')$ knowing the amount (μM) of fibrin that has been lyzed off the outside of the fibers, the lysis $L(x', t')$ is related to the number of fibrils (and equivalent volume) of the fiber degraded. Rearrangement of the equation below yields Eq. 14 in the text.

$$L(x', t') = [\pi R_{f_o}^2 - \pi R_f(x', t')^2]p_o\left(\frac{L_T}{\mathrm{Vol}_T}\right)\frac{2\ \text{monomers}}{45\ \text{nm}}\frac{1}{N_{av}}\frac{10^6\ \mu\text{mol/mol}}{10^{-3}\ \text{l/cm}^3}$$

The local bulk porosity can be defined with respect to the local fiber diameter since the length of fiber per unit volume remains constant during lysis:

$$\epsilon(x, t) = 1 - \frac{V_{\text{solid}}\ \text{in}\ \Delta V}{\Delta V} = 1 - \pi R_f(x', t')^2 \cdot \frac{L_{\Delta V}}{\Delta V} \cdot \left(10^{-21}\frac{\text{cm}^3}{\text{nm}^3}\right)$$

The local specific permeability $k(x, t)$ is calculated from ϵ(x, t) and $R_f(x, t)$ using Eq. 2. At any given time t', the overall specific permeability can be evaluated as the inverse of the total resistivity by integrating the local resistivity $[k(x, t')]^{-1}$ over the length of the clot.

The authors acknowledge the many helpful discussions and important insights offered by Drs. Johannes Nitsche and Ralph Yang. Also, the authors wish to thank Drs. Sal Pizzo, Don Gabriel, and Patrick McKee for their helpful insights on the biochemistry of fibrinolysis.
This research was supported by a National AHA Grant 93-8670 and NIH Grant HL47486-01A1. S. L. D. is the recipient of a National Science Foundation National Young Investigator Award.

REFERENCES

Bird, R. B., W. E. Stewart, and E. N. Lightfoot. 1960. Transport Phenomena. John Wiley and Sons, New York.

Bischoff, K. B. 1965. Effectiveness factors for general reaction rate forms. *AIChE J.* 11:351–355.

Blinc, A., G. Planinsic, D. Keber, O. Jarh, G. Lahajnar, A. Zidansek, and F. Demsar. 1991. Dependence of blood clot lysis on the mode of transport of urokinase into the clot-A magnetic resonance imaging study in vitro. *Thromb. Haem.* 65:549–552.

Blomback, B., and M. Okada. 1982. Fibrin gel structure and clotting time. *Thromb. Res.* 25:51–70.

Blomback, B., K. Carlsson, B. Hessel, A. Liljeborg, R. Procyk, and N. Aslund. 1989. Native fibrin gel networks observed by 3D microscopy, permeation, and turbidity. *Biochim. Biophys. Acta.* 997:96–110.

Blum, J. J., G. Lawler, M. Reed, and I. Shin. 1989. Effect of cytoskeletal geometry on intracellular diffusion. *Biophys. J.* 56:995–1005.

Bok, R. A., and W. F. Mangel. 1985. Quantitative characterization of the binding of plasminogen to intact fibrin clots, lysine-Sepharose, and fibrin cleaved by plasmin. *Biochemistry.* 24:3279–3286.

Brenner, H., and L. J. Gaydos. 1977. The constrained Brownian movement of spherical particles in cylindrical pores of comparable radius: models of the diffusive and convective transport of solute molecules in membranes and porous media. *J. Colloid Interface Sci.* 58:312–355.

Carr, M. E., and C. L. Hardin. 1987. Fibrin has larger pores when formed in the presence of erythrocytes. *Am. J. Physiol.* 253:H1069–H1073.

Carr, M. E., and C. L. Hardin. 1987. Large fibrin fibers enhance urokinase-induced plasmin digestion of plasma clots. *Blood.* 70:400 (Abstr).

Carr, M. E., and J. Hermans. 1978. Size and density of fibrin fibers from turbidity. *Macromolecules.* 11:46–50.

Carr, M. E., C. Krishnamurti, and B. Alving. 1992. Effect of plasminogen activator inhibitor-1 on tissue plasminogen activator-induced fibrinolysis. *Thromb. Haem.* 67:106–110.

Carr, M. E., L. L. Shen, and J. Hermans. 1977. Mass-length ratio of fibrin fibers from gel permeation and light scattering. *Biopolymers.* 16:1–15.

deVries, C., H. Veerman, and H. Pannekoek. 1989. Identification of the domains of tissue-type plasminogen activator involved in the augmented binding to fibrin after limited digestion with plasmin. *J. Biol. Chem.* 264:12604–12610.

Doolittle, R. F. 1984. Fibrinogen and fibrin. *Annu. Rev. Biochem.* 53: 195–229.

Dullien, F. A. 1979. Porous Media: Fluid Transport and Pore Structure. Academic Press, New York. 167.

Fears, R. 1989. Binding of plasminogen activators to fibrin: characterization and pharmacological consequences. *Biochem. J.* 261:313–324.

Gabriel, D. A., K. Muga, and E. M. Boothroyd. 1992. The effect of fibrin structure on fibrinolysis. *J. Biol. Chem.* 267:24259–24263.

Gupta, S. P., and R. A. Greenkorn. 1973. Dispersion during flow in porous media with bilinear adsorption. *Water Resources Res.* 9:1357–1368.

Haber, E., T. Quertermous, G. R. Matsueda, M. S., and Runge. 1989. Innovative approaches to plasminogen activator therapy. *Science (Washington DC).* 243:51–56.

Harpel, P. C., T. S. Chang, E. Verderber. 1985. Tissue plasminogen activator and urokinase mediate the binding of Glu-plasminogen to plasma fibrin I: evidence for new binding sites in plasmin-degraded fibrin I. *J. Biol. Chem.* 260:4432–4440.

Higgins, D., and G. A. Vehar.1987. Interaction of one-chain, and two-chain tPA with intact and degraded fibrin. *Biochemistry.* 26:7786–7791.

Hoylaerts, M., D. C. Rijken, H. R. Lihnen, and D. Collen. 1982. Kinetics of the activation of plasminogen by human tissue plasminogen activator. *J. Biol. Chem.* 257:2912–2919.

Hunziker, E. B., P. W. Straub, and A. Haeberli. 1990. A new concept of fibrin formation based upon the linear growth of interlacing and branching polymers and molecular alignment into interlocking single-stranded segments. *J. Biol. Chem.* 265:7455–7463.

Husain, S. S., A. A. K. Hasan, and A. Z. Budzynski. 1989. Differences between binding of one-chain and two-chain tissue plasminogen activators to non-cross-linked and cross-linked fibrin clots. *Blood.* 74: 999–1006.

Jen, C. J., and L. V. McIntire. 1986. Platelet microtubules in clot structure formation and contractile force generation. *Thromb. Haemostasis.* 56: 23–27.

Kaufman, E. N., and Jain, R. K. 1990. Quantification of transport and binding parameters using fluorescence recovery after photobleaching. *Biophys. J.* 58:873–885.

Kirkner, D. J., T. L. Theis, and A. A. Jennings. 1984. Multicomponent solute transport with sorption and soluble complexation. *Adv. Water Res.* 7: 121–125.

Lijnen, H. R., B. Van Hoef, F. De Cock, and D. Collen. 1989. The mechanism of plasminogen activation and fibrin dissolution by single chain urokinase-type plasminogen activator in a plasma milieu in vitro. *Blood.* 73:1864–1872.

Lottenberg, R., U. Christensen, C. M. Jackson, and P. L. Coleman. 1981. Assay of coagulation proteases using peptide chromogenic and fluorogenic substrates. *Methods Enzymol.* 80:341–361.

Lucas, M. A., L. J. Fretto, and P. A. McKee. 1983. The binding of human plasminogen to fibrin and fibrinogen. *J. Biol. Chem.* 258:4249–4256.

Matveyev, M. Y., and S. P. Domogatsky. 1992. Penetration of macromolecules into contracted blood clots. *Biophys. J.* 63:862–863.

Miles, L. A., and Plow, E. F. 1985. Binding and activation of plasminogen on the platelet surface. *J. Biol. Chem.* 260:4303–4311.

Nair, C. H., and A. Azhar, J. D. Wilson, and D. P. Dhall. 1991. Studies of fibrin network structure in human plasma. Part II. Clinical application: diabetes and antidiabetic drugs. *Thromb. Res.* 64:477–485.

Park, I. H., C. S. Johnson, M. R. Jones, and D. A. Gabriel. 1988. Probes of fibrin gel porosity. *Proc. Int. Fibrinogen Workshop.* 3:123–126.

Phillips, R. J., W. M. Deen, and J. F. Brady. 1990. Hindered transport in fibrous membranes and gels: effect of solute size and fiber configuration. *J. Coll. Interface Sci.* 139:363–373.

Pizzo, S. V., M. L. Schwartz, R. L. Hill, and P. A. McKee. 1973. The effect of plasmin on the subunit structure of human fibrin. *J. Biol. Chem.* 248: 4574–4583.

Ranby, M., and A. Brandstrom. 1988. Control of t-PA mediated fibrinolysis. *In* Tissue-type Plasminogen Activator (t-PA). C. Kluft, editor. CRC Press, Boca Raton, FL. 211–224.

Robbins, K. C., L. Summaria, D. Elwyn, and G. H. Barlow. 1965. Further studies of the purification and characterization of human plasminogen and plasmin. *J. Biol. Chem.* 240:541–550.

Robbins, K. C., L. Summaria, and R. C. Wohl. 1981. Human plasmin.

Methods Enzymol. 80:379–387.

Rubin, J. 1983. Transport of reacting solutes in porous media: relation between mathematical nature of problem formulation and chemical nature of reactions. *Water Resources Res.* 19:1231–1252.

Sabovic, M., H. R. Lijnen, D. Keber, and D. Collen. 1989. Effect of retraction on the lysis of human clots with fibrin specific and non-fibrin specific plasminogen activators. *Thromb. Haemostasis.* 62:1083–1087.

Sabovic, M., H. R. Lijnen, D. Keber, and D. Collen. 1990. Correlation between progressive adsorption of plasminogen to blood clots and their sensitivity to lysis. *Thromb. Haemostasis.* 64:450–454.

Sahimi, M., B. D. Hughes, L. E. Scriven, and H. T. Davis. 1986. Dispersion in flow through porous media—one-phase flow. *Chem. Eng. Sci.* 41: 2103–2122.

Sobel, B. E., R. W. Gross, and A. K. Robison. 1984. Thrombosis, clot selectivity, and kinetics. *Circulation.* 70:160–164.

Suenson, E., and S. Thorsen. 1981. Secondary-site binding of Glu-plasmin, Lys-plasmin, and miniplasmin to fibrin. *Biochem. J.* 197:619–628.

Tiefenbrunn, A. J., R. A. Graor, A. K. Robinson, F. V. Lucas, A. Hotchkiss, and B. E. Sobel. 1986. Pharmocodynamics of tissue-type plasminogen activator characterized by computer-assisted simulation. *Circulation.* 73: 1291–1299.

Tyn, M. T., and T. W. Gusek. 1990. Prediction of diffusion coefficients of proteins. *Biotech. Bioeng.* 35:327–338.

Weisel, J. W., and C. Nagaswami. 1992. Computer modeling of fibrin polymerization kinetics correlated with electron microscope and turbidity observations: clot structure and assembly are kinetically controlled. *Biophys. J.* 63:111–128.

Whitaker, S. Mass transport, and reaction in catalyst pellets. 1987. *Transport Porous Media.* 2:269–299.

Wu, H. L., Chang, B. I., Wu, D. H., Chang, L. C., Gong, C. C., Lou, K. L., and Shi, G. Y. 1990. Interaction of plasminogen and fibrin in plasminogen activation. *J. Biol. Chem.* 265:19658–19664.

Zidansek, A., and A. Blinc. 1991. The influence of transport parameters and enzyme kinetics of the fibrinolytic system on thrombosis: mathematical modelling of two idealised cases. *Thromb. Haem.* 65:553–559.